NSIRC RESEARCH & INNOVATION CONFERENCE 2023

TWI Ltd, Cambridge, UK | 14-15 June 2023

Industry-Led Postgraduate Research Solving Global Technology Challenges

WWW.NSIRC.CO.UK/CONFERENCE2023

Official Event Sponsors 2023

BLAZE

by AeonX

QUANTUM-SAFE END-TO-END ENCRYPTED DATA SHARING

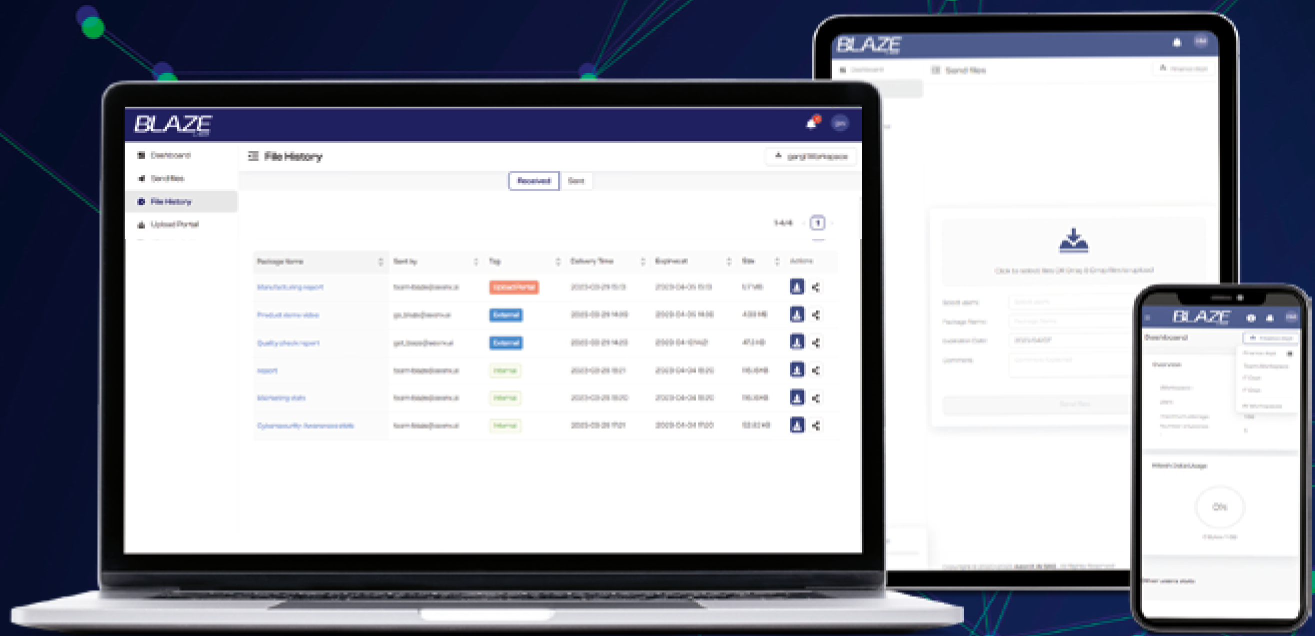

"Zero-Trust" security of Blaze Transfer ensures that only the sender and the recipients can decrypt the data, granting exclusive access to the shared data.

Securely share your research and industrial data with your teams and clients.

- Zero-Trust security
- Transfer TBs of data, fast
- Organisation workspace

Co-funded by the EU.
GA No.: 101058179

https://blaze.cx

Brunel University London

UKRI Innovate UK

CARRS WELDING TECHNOLOGIES LTD

AILU ASSOCIATION OF INDUSTRIAL LASER USERS

SONI-LASER

Ultrasonic assisted laser welding for high volume assembly of automotive battery packs

Electric Vehicle Batteries

Electric vehicle sales will reach 44 million vehicles per year by 2030. Therefore, there is an increasing need for the manufacturing of battery packs to meet demand. Whilst Asia remains the stronghold (projected to reach 800GWh by 2025), Europe is expanding rapidly with a projected production capacity of 450GWh/year by 2030

Laser Welding

Laser welding has emerged as the optimal welding technique for EV battery manufacturing; being 4-5 times faster than the current welding processes. While laser welding is well suited to the increasing manufacturing demand and the joining needs of the battery pack assembly, challenges to its application in this industry remain.

UltraSonic Vibration Treatment

Making the required joints represent several metallurgical challenges, including, joining of multiple dissimilar materials of varying thicknesses. SoniLaser will introduce a Power-Ultrasonic Vibration Treatment that will assist the laser welding process of EV batteries in order to enhance the integrity and quality of welds.

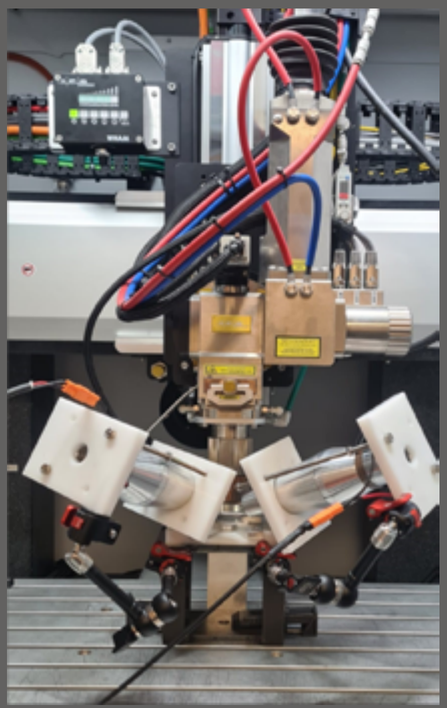

01536 412828
pc@carrswelding.co.uk
samiul@carrswelding.co.uk
https://carrswelding.co.uk/

CYBER ESSENTIALS CERTIFIED

nqa ISO 14001 ENVIRONMENTAL MANAGEMENT — UKAS MANAGEMENT SYSTEMS 0015

nqa ISO 9001 QUALITY MANAGEMENT — UKAS MANAGEMENT SYSTEMS 0015

Brunel Innovation Centre

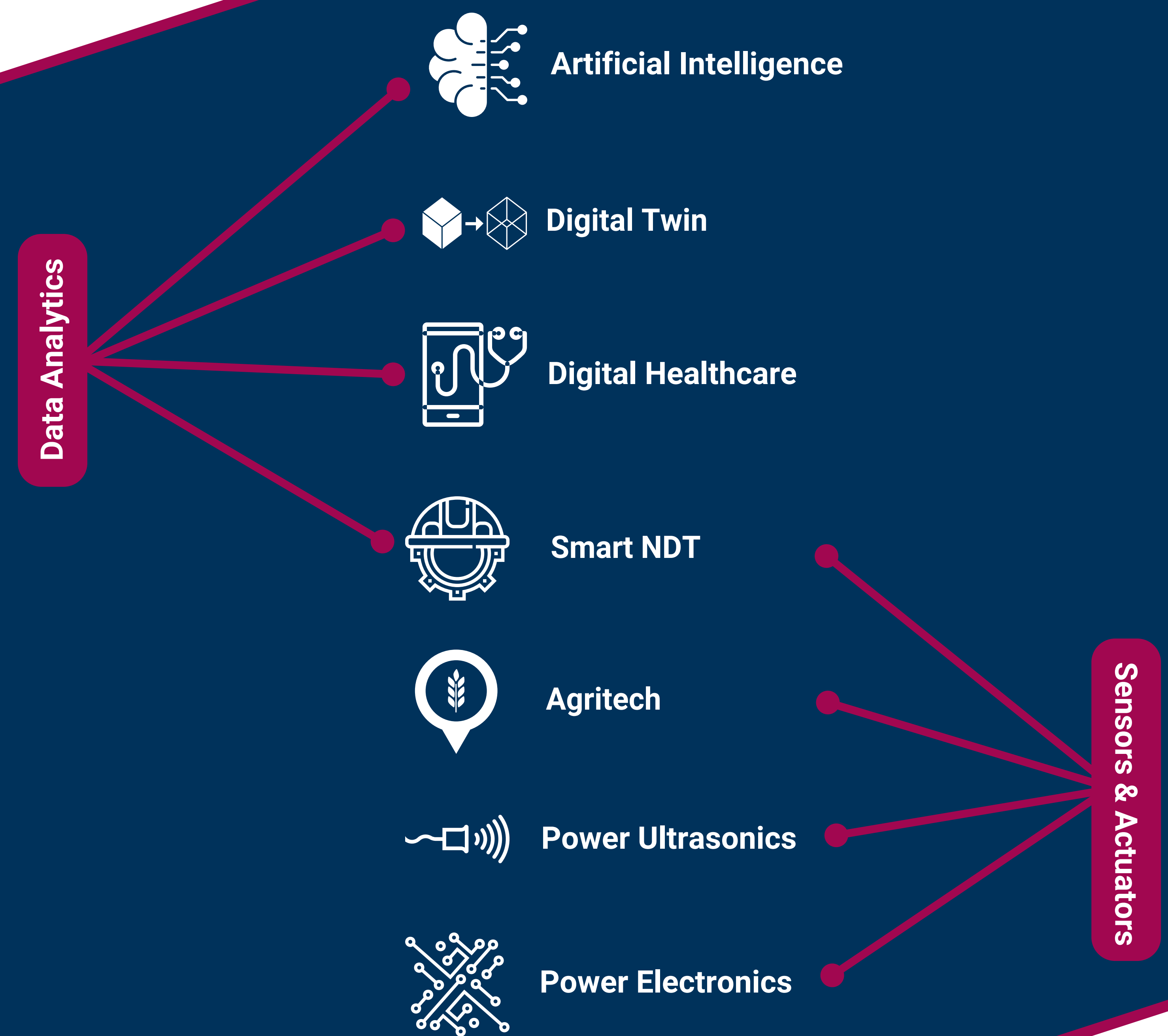

bicqueries@brunel.ac.uk

Brunel Composites Centre

Developing innovative methods for composite processing and joining for the industry

The Brunel Composites Centre (BCC) creates shared research and technology capabilities, specialising in novel composites processing and joining technologies applied to industrial environments.
The Centre has developed a financially sustainable research facility, drawing on existing strengths at Brunel University London to complement and underpin applied research and development activities at TWI Ltd where the centre is based.

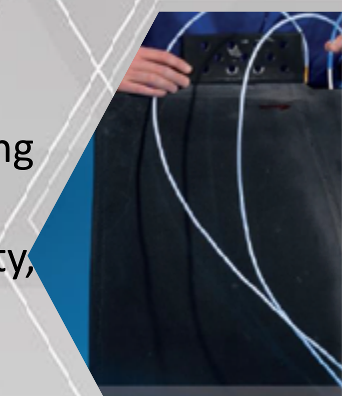

For further information, please contact us:

bcc@brunel.ac.uk
https://www.brunel.ac.uk/research/centres/brunel-composites-centre
Brunel Composites Centre (BCC)
Granta Park, Great Abington
Cambridge
CB21 6AL
United Kingdom

WELCOME FROM PROF TAT-HEAN GAN

NSIRC RESEARCH & INNOVATION CONFERENCE 2023

Tat-Hean

Professor Tat-Hean Gan
NSIRC Director
TWI Director, Membership, Innovation & Global Operations

A warm welcome to TWI Cambridge, UK for this year's two-day NSIRC Research and Innovation Conference, as well as the TWI Innovation Network Convention 2023 which runs concurrently to it on Thursday 15 July! As in previous years, we hope that delegates will benefit from the cross-fertilisation of research and innovation activities, and industry-academia networking that these two events make possible.

In what has been a successful year to date, 2023 has seen further evolution of the National Structural Integrity Research Centre (NSIRC) as it continues to establish and expand its presence overseas through NSIRC International. A number of universities spanning Thailand, Greece, Malaysia, Indonesia and India have now signed Memorandums of Understanding (MoUs) with TWI, with the aim of creating novel PhDs that reflect industrial needs in their respective regions. The first NSIRC International students have now started their research studies and recruitment is ongoing as awareness of the international programme continues to grow. We are also pleased to report that Manchester Metropolitan University (MMU) in the UK, and TWI's partner in the Advanced Manufacturing and Digitalisation Innovation Centre, have co-signed an MoU in relation to NSIRC International in Thailand.

Our thanks are extended to Lloyd's Register Foundation, one of the foundering partners of NSIRC alongside bp plc and TWI back in 2012, whose ongoing support and expertise are invaluable in establishing and growing NSIRC International.

Simultaneously, NSIRC in the UK continues to go from strength to strength, currently offering industry-focused PhDs and MScs as well as the Senior Leader (Executive) Apprenticeship awarded by De Montfort University, and the recently introduced Engineering CPD Courses awarded by longstanding NSIRC partner Brunel University London..

Below are a selection of NSIRC's latest achievements that we would like to share with you:

- **191 PhDs** and **170 MScs** students undertaking postgraduate research in an industrial setting to advance their knowledge and make scientific breakthroughs
- **100% employment rate** for PhD students within one year of graduating
- **Females represent 32%** of NSIRC PhD students, compared to a UK engineering workforce female representation of 16.5%
- A network of more than **45 university partners**, via signed agreements, in the UK and overseas
- MoUs signed with **8 universities in 6 countries** under the NSIRC International Programme
- **£150m** invested in facilities, equipment and studentships
- **880+** publications
- **13 standards** updates contributed to by NSIRC research
- Ongoing engagement with the **ASEAN Committee on Science and Technology** for potential collaboration with Indonesia and the Philippines

Lastly, I hope you enjoy this year's in-person event, and will join me in congratulating the NSIRC students on their outstanding work which they look forward to sharing with you during the conference.

Photo: Unsplash / New York Public Library

DPS_9535 0720

KEYNOTE SPEAKERS

Dr Tim Slingsby

Director, Skills & Education
Lloyd's Register Foundation

In his role at the Foundation, Tim is involved in working with an international network of HE, NGO, IGO and industry professionals to manage, direct and communicate issues and research that have an impact on society. Alongside this, he is serving as the Chair at Maritime Charities Group.

Before joining LRF, Tim worked in the science team at the British Council, the UK's international organisation for cultural relations and educational opportunities, where he was responsible for public engagement and STEM education that impacts. In addition, he studied Human Genetics at the University of Nottingham and holds a PhD in Molecular Genetics from the University of Leicester.

Dr Christina Guindy

Associate Director,
Research Programmes & Awards
Royal Academy of Engineering

In her role at RAEng, Christina is responsible for the distribution of awards and grants that aim to promote talent and innovation for the benefit of society, and she has taken steps to make sure diversity and inclusion are integral parts of this process.

Before joining the Academy, Christina was a founding staff member of KAUST (King Abdullah University of Science and Technology, in Saudi Arabia) and was heavily involved in creating global partnerships with other institutions. She also served as Assistant Dean, helping to grow and maintain the Physical Science and Engineering Division at KAUST. She has also worked at the EPSRC to encourage collaboration between academia and industry.

Stuart Broadley FEI

Chief Executive Officer,
Energy Industries Council (EIC)

Stuart joined the EIC back in 2016 and took up the position of CEO following a successful 25-year career leading global businesses in oil and gas, power, renewables, and defence.

In 2023, the EIC was honoured with the King's Award for International Trade. The council is impartial regarding energy sources and is currently one of the largest energy trade associations worldwide, boasting over 900 member companies.

Stuart holds the position of co-chair for the UK Energy Supply Chain ministerial taskforce and serves as the Energy co-chair for the UAE-UK Business Council. He has played a key role in organising the Energy Exports Conference, which has successfully attracted 20 delegations to the UK. Additionally, he is the author of the Survive & Thrive annual reports, which provide valuable insights into preferred growth strategies for challenging markets.

ABOUT NSIRC

NSIRC (National Structural Integrity Research Centre) is a state-of-the-art postgraduate engineering facility, established and managed by structural integrity specialist TWI Ltd, with the aim of becoming the world centre for structural integrity research.

The centre was founded in 2012 by industrial partners TWI, Lloyd's Register Foundation and bp plc, as well as lead academic partner Brunel University London.

Since then, NSIRC has collaborated with over 45 world-leading universities with capability to deliver high quality research that can address complex industrial challenges.

These affiliated university partners provide academic excellence to address the need for fundamental research, and industry partners provide high-quality, industry-relevant training, for the next generation of structural integrity engineers.

The mission of NSIRC is to advance fundamental research that will:

- Support the safe operation of products and structures
- Develop innovative, fit-for-purpose technologies and design rules
- Demonstrate solutions for long-term asset management

This includes risk-based management, engineering critical assessment, non-destructive testing, structural health and condition monitoring, and health management for use in real world settings.

101

PhDs successfully completed

35

Number of countries students come from to NSIRC

£150m

Invested in PhD research facilities, equipment and studentships

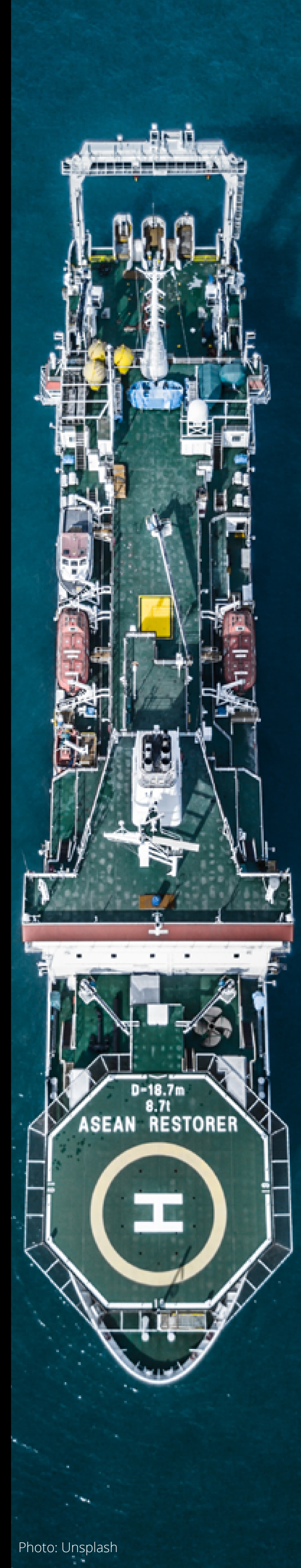

Photo: Unsplash

Strategic partnership between ARU and TWI Limited

The Anglia Ruskin Innovation Centre (ARIC) aims to develop a comprehensive research capacity, focussed on digital transformation of management, people, skills and organisational innovation.

ARIC will:

- Establish a reputation of excellence and be among the world leaders in industrially relevant digital transformation and innovation management research, driving innovation and sustainable economic growth
- Use research and development to create the next generation of business models and tools to commercialise technologies, benefit TWI industrial members and address societal challenges
- Drive new regional research and technology capability for the acceleration of digital adoption
- Undertake joint research programmes and secure a portfolio of research funding from external sponsors.

To find out how our research and development can help your business break formation and accelerate

Call **01223 695878**
Email **business@aru.ac.uk**
Visit **aru.ac.uk/business-employers**

Every partnership starts with a conversation

Start your conversation Today

@ARUBusiness
ARU Enterprise and Innovation

a.r.u. Anglia Ruskin University

AFFILIATED UNIVERSITIES

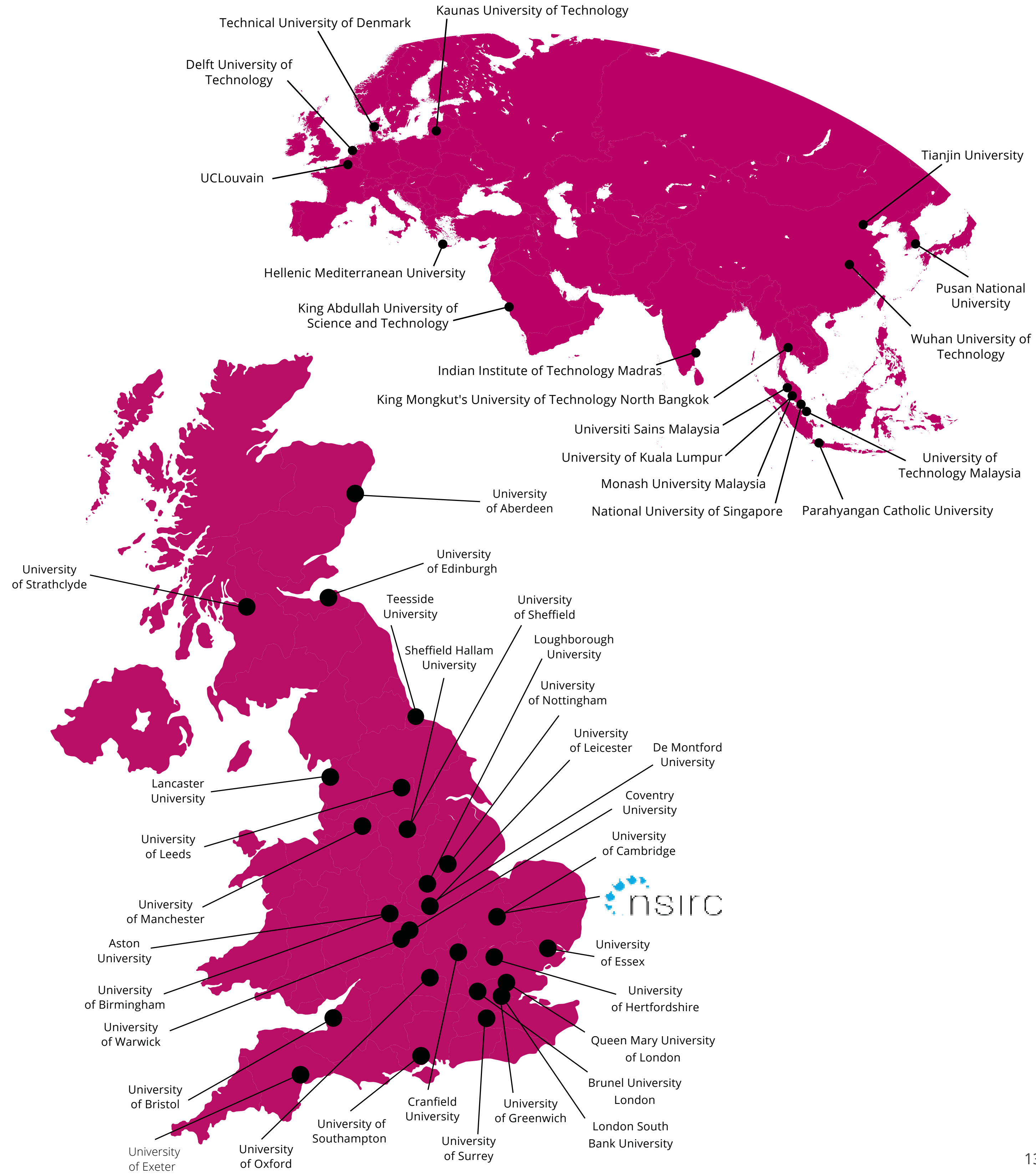

DAY 1 AGENDA

Day 1 - 14th June

09:00 Arrival and Refreshments

09:30 Introduction and Welcome
Prof Tat-Hean Gan, Director NSIRC

09:50 **Keynote Speaker**
Engineering Capabilities Where They Are Most Needed
- Tim Slingsby, Director of Skills and Education at Lloyd's Register Foundation and Chair of Maritime Charities Group

Structural Integrity sponsored by Brunel University London

10:20 First principles validation of barriers in NiAl - *Adam Fisher*

10:45 Thermal-mechanical analysis of mixing points in nuclear power plants - *Funke Dacosta-Salu*

11:10 Break

11:35 Numerical analysis of welding residual stresses in a T-joint fillet weld - *Anurag Niranjan*

12:00 Sensitivity analysis of magnetic circuit components of magnetic flux leakage device for appropriate magnetisation - *Selamawit Abate*

12:25 Sensitivity of neutrons to hydrogen in steels - *Soumyadeep Datta*

12:50 Lunch, Networking and Exhibition

Joining Technologies sponsored by Brunel Composites Centre

14:00 Composite-to-metal joining for naval vessels - *Man Chi Cheung*

14:25 Human-robot collaboration for braze pasting workflow - *Haolin Fei*

14:50 Weld quality assessment of FSW joints by continuous acoustic emission monitoring - *Kartikey Mathur*

15:15 Poster Session - Break

Robotics & Artificial Intelligence sponsored by Brunel Innovation Centre

15:50 Learning by demonstration for learning complex manipulation strategies directly from pixels - *Antonios Porichis*

16:15 Bridging the Simulation to Reality Gap in Robotics - *Konstantinos Vasios*

16:40 Multi-response optimization and web-based visualization of Ti6Al4V support structures for laser powder bed fusion systems - *Antonios Dimopolous*

17:05 **Closing Words**

End of Day 1

DAY 2 AGENDA

Day 2 - 15th June

09:00 Arrival and Refreshments

09:30 Introduction and Welcome

09:35 **Keynote speaker**
Royal Academy of Engineering: Priorities & Opportunities
- Dr Christina Guindy, Associate Director, Research Programmes & Awards at Royal Academy of Engineering

Additive Manufacturing sponsored by Anglia Ruskin University

10:05 Structural integrity assessment of cold spray repaired high-strength aluminium alloy 7075 specimens - *Ali Alperen Bakir*

10:30 Wire-fed DED of low carbon steels – influence of process control methods on properties and microstructure - *Ahamed Ameen*

10:55 Break

11:20 Examination of environmental cracking in additively manufactured materials - *Yixiang Jin*

11:45 Effect of process parameters on bead geometry of low carbon alloy steel manufactured by wire arc directed energy deposition (DED) - *Siddharth Patil*

12:10 Development of post thermal treatments for L-PBF A20X - *Francesco Careri*

12:35 Lunch

13:30 **Keynote Speaker**
Setting The Scene – Understanding The Changing Energy Market
- Stuart Broadley, CEO, Energy Industries Council (EIC)

Coatings Technologies sponsored by University of Leicester

14:00 Investigating mechanical performance of self piercing rivet (SPR) joint for dissimilar materials joints - *Muhammad Haris*

14:25 Electrochemical determination of hydrogen diffusion using devanathan-stachurski cell - *Arunima Bhuvanendran Nair Jayakumari*

14:50 The optimisation of Ni superalloy coatings using extreme high-speed laser application (EHLA) technology - *David Satterlee*

15:15 Break

15:40 Introduction of solvent de-curing trigger to enable dissolution of epoxy thermoset - *Magali Rego*

16:05 Real-time optical and electrochemical monitoring of extreme damage tolerant sacrificial coatings - *Adriana Castro Vargas*

16:30 **Awards & Closing Words**

16:45 **Award Winner Photos & Closing**

Adam Fisher

I am a third year PhD student based at the University of Warwick. I am part of the HeySys CDT. I graduated from Loughborough University with a Masters in Computer Science and Mathematics. My area of research is in NiAl superalloys looking at the development of phases and the rate of their growth. This publication was made possible by the sponsorship and support of the Core Research Programme, a market-driven programme of research and development activities that underpin the creation and optimisation of joining, materials and engineering technologies. The work was enabled through, and undertaken at, the National Structural Integrity Research Centre (NSIRC), a postgraduate engineering facility for industry-led research into structural integrity established and managed by TWI.

First principles validation of barriers in NiAl

Huan Wu[1], Tyler London[1], Peter Brommer[2], Julie Staunton[2]
[1]TWI, [2]University of Warwick
3rd Year of PhD

Keywords: Nickel-based superalloys, bottom-up approach, kinetic Monte Carlo

I. INTRODUCTION

High temperatures are the domain of the superalloys as they retain all their desirable properties at a high percentage of their melting point[1]. Nickel-based superalloys are used for their resistance to fatigue and creep, coupled with their strength. Retaining these properties at a higher temperature range than other alloys is why these types of superalloys are usually chosen. Control of the alloy structure at the microscopic level is required to guarantee these properties. The microstructure of nickel-based superalloys has many different phases, and these phases contribute to the properties that make superalloys so useful.

Nickel Aluminium superalloys are heat treated to facilitate the growth of these phases. Precipitate growth rates on a fundamental scale are governed by the motion of atoms arranging themselves in the correct fashion. Atomistic models could be used to inform simulations on longer length scales for a bottom-up approach. However, to have accurate atomistic models, we need to know how accurate our methods of obtaining energy values are.

II. DESIGN/METHODOLOGY/APPROACH

Given the times scales of precipitate growth, we have chosen kinetic Monte Carlo (kMC)[2] to study them. This allows us to accelerate simulation time, when compared to direct simulation of atomic motion with molecular dynamics, by jumping from state to state. Knowledge of energy barriers separating states is required and there a many method to find these. Here, we validate the barriers found using a kMC code against density functional theory (DFT), a first-principles method. This is to assess how accurate the much faster interatomic potential is against the expensive but accurate DFT.

We evolved the system over 500 kMC steps at 900 K using the off-lattice, self-learning kMC code kART[3], which uses an open-ended saddle point search technique to find energy barriers. Energy calculations are made using LAMMPS[4] using Pun-Mishin 2009[5] interatomic potential through OpenKIM[6]. In this way, we obtain 500 events. From initial and final states of these events, we re-evaluate the barrier heights using the nudged elastic band (NEB) method using the same effective potential. This serves two purposes: Firstly, we validate kART barrier heights against another method. Secondly, it allows us to re-calculate the barriers using first principles as outlined below. Multi-atom events were excluded as they do not transfer well to the smaller cells later on and the barriers are unstable to decompose into multiple events. We also only consider distinct event as some events are found several times during the kMC run. This reduces the number of events down to 87 distinct events.

For the next step, smaller cells are required to be able to calculate barriers using NEB with DFT. This is due to the computational complexity of DFT scaling very poorly with the number of atoms. The process of cutting down to a smaller cell is achieved by first centering on the moving atom and then cutting down to 4 x 4 x 4 unit cells. We then perform an effective potential NEB with consistent settings to see what effects the process has had on the barrier heights.

Our final step is to compare these reduced-cell energy barriers with a CASTEP DFT NEB. Due to the computational complexity of DFT calculations, only a limited number of barriers can be compared in this way.

We focus on events that share an initial state but have different final configurations. These are used to see if the relative ordering of barriers is maintained, as a change in ordering would affect the probability of being picked.

III. FINDINGS/RESULTS

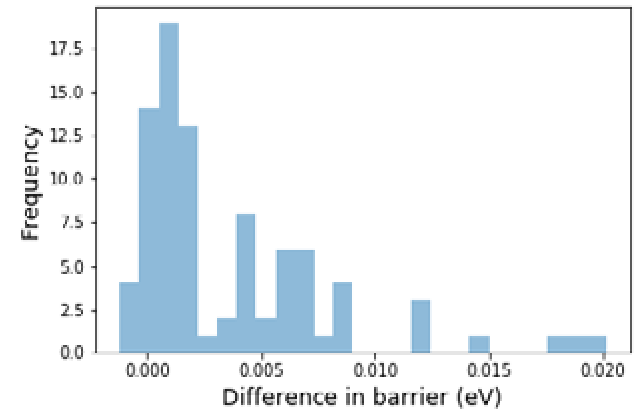

Figure 2
Difference between distinct barriers values found using kART and NEB.

When comparing barrier values obtains from kART and NEB we get very good agreement between the 2 different methods. It can be seen from Fig. 2. that at maximum there is a difference between methods of 0.02eV or maximum percentage error of 3.2% with most differing by much less than that. This level of agreement shows that the two methods produce consistent results.

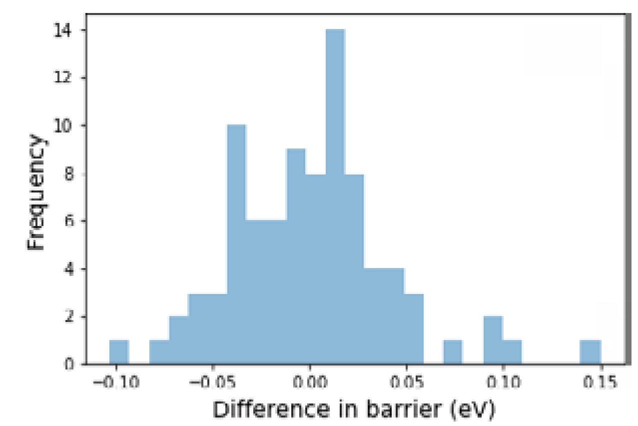

Figure 3
Difference between distinct barriers in cells of size 8x4x4 and 4x4x4

As shown in Fig. 3, reducing the cell size changes the barriers by up to 0.15 eV. This shows that the events we studied can be reasonably evaluated in the smaller simulation cell.

Moving on to looking at the differences between the effective potential and DFT. Most barriers show around a −0.3 eV difference as can be seen in Fig. 4. If this was the case for all barriers, we would still see the correct kinetics in kMC but altered time scales. However, for one starting state, the order of a pair of barriers switches, with the effective potential and DFT disagreeing on which one has the lower barrier height. This means using this potential could give us different kinetics as what once was the most probable barrier is now less probable than another one. This could lead the system to evolve in a completely different direction, although this is not guaranteed.

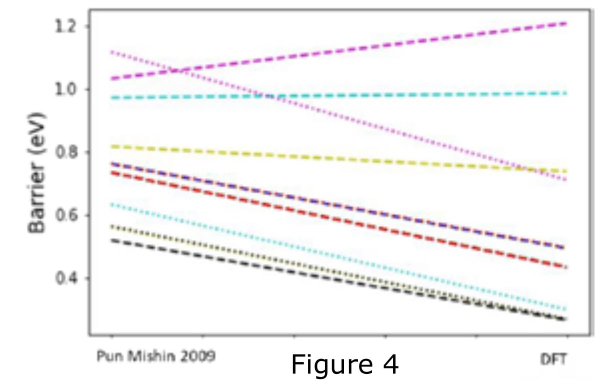

Figure 4
How barrier heights change from interatomic potential to DFT. Same colour indicates shared initial state

IV. DISCUSSION/CONCLUSIONS

The interatomic potential may not be suitable for our purpose due to the inaccuracies in the barrier values for certain barriers. However, we have shown that kART and NEB find consistent barrier heights. In the process, we have created a valuable tool chain to study and validate events and barriers used to model precipitate evolution in alloys. We also demonstrated the use of this tool chain for NiAl superalloys.

V. FUTURE PLAN/DIRECTION

Our next steps are to find a potential suitable for our needs. This could be other already available interatomic potential or a machine learned one. After this we are looking to use kMC to find growth rates of precipitates for varying temperatures and concentrations of Al to allow us to optimisation of the alloy nanostructure.

REFERENCES

[1] C. T. Sims, Superalloys, vol. 1984, pp. 399-419, 1984
[2] A F Voter, Springer Netherlands, 2007.
[3] N. Mousseau et al., Journal of Atomic and Molecular Physics, vol. 2012, (2012)
[4] LAMMPS, A. P. Thompson, H. M. Aktulga, R. Berger, D. S. Bolintineanu, W. M. Brown, P. S. Crozier, P. J. in 't Veld, A. Kohlmeyer, S. G. Moore, T. D. Nguyen, R. Shan, M. J. Stevens, J. Tranchida, C. Trott, S. J. Plimpton, Comp Phys Comm, 271 (2022) 10817
[5] G. Purja Pun and Y. Mishin, Philosophical Magazine, vol. 89, no. 34-36, pp. 3245-3267, (2009)
[6] 4 E. B. Tadmor, R. S. Elliott, J. P. Sethna, R. E. Miller and C. A. Becker JOM, 63, 17 (2011)

Funke Dacosta-Salu

I studied Mechanical Engineering at Obafemi Awolowo University, Nigeria, and Loughborough University, United Kingdom for my Undergraduate and Master courses respectively. Subsequently, I worked as a Mechanical Engineer in the Building service sector for two years and I moved to the Oil and Gas sector where I worked for about three years as a senior subsea and pipeline engineer and technology development lead before starting my PhD with Coventry University as a Lloyds Foundation Register scholar.

Thermal-mechanical analysis of mixing points in nuclear power plants

Funke Dacosta-Salu[1,2], Micheal E Fitzpatrick[2], Xiang Zhang[2], Tyler London[3], Alessio Basso[3], and James Jewkes[4]
[1]NSIRC, TWI Ltd, [2]Coventry University, [3]TWI, [4]University of Leicester
3rd Year of PhD

Keywords: Temperature fluctuation, thermal fatigue, mixing points, T-junction, computational fluid dynamics, finite element analysis

I. INTRODUCTION

Thermal fatigue has been a concern in many industries for years, especially in the nuclear and energy sectors. Despite the implemented mitigation measures, a total number of 13 failures (through-wall cracks) due to thermal fatigue were recorded in the pressurized water reactor (PWR) in nuclear power plants. These leakages occurred at different ages of the reactors' usage [1]. Thermal fatigue has been considered an aging problem. However, damages, such as through-wall cracking in Civaux 1, France, 1998, occurred after only 1500h of operation of the pressurized water reactor, suggest that thermal fatigue should be critically analysed. This particular episode lead to more focused attention to thermal fatigue phenomena in T-junctions [2, 3]. Mixing points have been identified as locations potentially susceptible to thermal fatigue. A mixing point (also referred to as a T-junction) is a localised regions within the pipe section, where two or more fluids of different temperatures mix and flow together in the same direction. T-junctions are very common in industrial plants where flow mixing is required, for instance, to locally dissipate heat. The turbulent mixing of these fluids at different operating temperatures and mass flow rates leads to significant temperature and pressure fluctuations in the vicinity of a mixing point. This effect is commonly known as thermal striping [4]. When thermal striping occurs, high magnitude, low-frequency (0.1 -10 Hz) thermal fluctuations in the fluid propagate through the pipe wall, inducing a stress range [2]. If the stress range variation is above the fatigue limit of the material of the pipe, cracks could potentially initiate and propagate within a few cycles of operation. The fatigue limit is the stress threshold under which the material can undergo an infinite number of load cycles without experiencing fatigue. A method of preventing failure could be to ensure proper and adequate checks are undertaken at a pre-determined inspection frequency. The objective of this research is to understand the combined effect of structural constraints and operating conditions on the fatigue life of pipelines, in order to recommend a structured procedure to monitor and inspect T-junctions susceptible to thermal fatigue.

II. DESIGN/METHODOLOGY/APPROACH

The proposed methodology in this research involves numerical analysis to understand the phenomena involving thermal fatigue at mixing points. The numerical methodology consists of a sequentially-coupled Fluid-Structure-Interaction (FSI) analysis. This research makes use of both Computational Fluid Dynamics (CFD) and Finite Element Analysis (FEA) to predict the thermal and mechanical field occurring during flow mixing that can result in fatigue. CFD analysis is used to determine the transient thermal field at the pipe inner walls. Temperatures are then mapped into the FEA solver to determine the subsequent stress and strain fields. A Design of Experiment (DOE) study is currently being undertaken to determine the sensitivity of the numerical solution with respect to the operating conditions and the structural constraints, in order to develop a knowledge framework that can help to support informed decisions on the appropriate inspection and monitoring procedures in the nuclear power industry.

III. FINDINGS/RESULTS

Turbulent mixing of hot and cold water at the mixing point resulted in incomplete mixing of the fluids in the vicinity of the mixing point. The mean and fluctuating components of velocity and temperature from CFD simulations have been compared with data from literature and are in good agreement. Frequency analysis of the temperature fluctuation was undertaken. This is to identify the frequency that contain the most energy. Although no clear peak was identified in the power spectrum analysis, the current study has identified that the largest energy content in the frequency range is between 0.1 and 10 Hz. Furthermore, structural analysis is undertaken to determine the relevant stress range and strain field produced, as a result of the thermal fluctuations.

IV. DISCUSSION/CONCLUSIONS

The turbulent flow of two fluids of different temperatures mixing at the T-junction has been investigated and the results compared with other numerical and experimental outcomes. The preliminary CFD results of this study are in good agreement with the experimental and numerical data from other publications in the literature. Locations of high-temperature fluctuations have been identified. These locations are in close proximity to the mixing point region.

V. FUTURE PLAN/DIRECTION

The next steps of this research involve the assessment of the thermal stress and strain and subsequent fatigue life, as proposed below.

1. Determine realistic stress fluctuations in the pipe based on the temperature fluctuations obtained from previous steps.

2. Carry out thermal fatigue analysis.

3. Compare results with the existing literature.

4. A parametric study with respect to flow operating conditions (e.g. inlet temperature, inlet velocity, operating pressure, etc.) and structural constraints to understand the effect on the final fatigue cycle and to generate knowledge that can better inform about inspection approach and frequency.

ACKNOWLEDGEMENT

THIS PUBLICATION WAS MADE POSSIBLE BY THE SPONSORSHIP AND SUPPORT OF LLOYD'S REGISTER FOUNDATION. THE WORK WAS ENABLED THROUGH, AND UNDERTAKEN AT, THE NATIONAL STRUCTURAL INTEGRITY RESEARCH CENTRE (NSIRC), A POSTGRADUATE ENGINEERING FACILITY FOR INDUSTRY-LED RESEARCH INTO STRUCTURAL INTEGRITY ESTABLISHED AND MANAGED BY TWI THROUGH A NETWORK OF BOTH NATIONAL AND INTERNATIONAL UNIVERSITIES. LLOYD'S REGISTER FOUNDATION HELPS TO PROTECT LIFE AND PROPERTY BY SUPPORTING ENGINEERING-RELATED EDUCATION, PUBLIC ENGAGEMENT AND THE APPLICATION OF RESEARCH. HTTP://WWW.LRFOUNDATION.ORG.UK/

REFERENCES

[1] C .L. Atwood, V. N. Shah, and W. J. Galyean, "Analysis of Pressurized Water Reactor Primary Coolant Leak Events Caused by Thermal Fatigue," in ESREL '99 - European Safety and Reliability, 1999.
[2] S. Chapuliot, C. Gourdin, T. Payen, J.P. Magnaud, A. Monavon, "Hydro-thermal-mechanical analysis of thermal fatigue in a mixing tee," Nuclear Engineering and Design 235, vol. 235, p. 575–596, 2005.
[3] M. Dahlberg, K.-F. Nilsson, N. Taylor, C. Faidy, U. Wilke, S. Chapuliot, D. Kalkhof, I. Bretherton, M. Church, J. Solin, and J. Catalano, "Development of a European Procedure for Assessment of High Cycle Thermal Fatigue in Light Water Reactors: Final Report of the NESC-Thermal Fatigue Project," Institute for Energy, Petten, 2011.
[4] I. S. JONES, "An Impulse Response Model for the Prediction of Thermal Striping Damage," Engineering Fracture Mechanics, vol. 55, pp. 795-812, 1996.

Anurag Niranjan

Anurag is a third year PhD student at Coventry University and NSIRC by the sponsorship and support of Lloyd's Register Foundation. He completed his M.Tech in Metallurgical engineering and Material sciences from Indian Institute of Technology Bombay. Before perusing PhD he has worked as a Failure Analysis Engineer for almost five year at Element, Abu Dhabi. His PhD (started in September 2020) focuses on studying a surface-breaking flaw at the weld toe region in a fillet weld under cyclic load using both numerical modelling and residual stress measurement at pre-defined crack depths. The outcome of this project will inform integrity assessment with respect to the treatment of residual stress in fillet welds and will be greatly beneficial for flaw tolerance assessments (BS 7910, API 591).

Numerical analysis of welding residual stresses in a T-joint fillet weld

Yin Jin[1], Jazeel chukkan[1], Michael Fitzpatrick[2], Niall Smyth[2]
[1]TWI, [2]Coventry University
3rd Year of PhD

Keywords: Weld modelling, Goldak's double ellipsoid heat source, weld residual stress

I. INTRODUCTION

Arc welding is a heavily employed joining process in various industries, including automotive, marine, and ship building. Understanding the thermal behaviour during welding is crucial for predicting weld bead geometry, residual stresses, and distortion. To accomplish this, numerical simulations have become a valuable tool. In this article, we delve into the world of weld modelling, focusing on heat source models, with a particular emphasis on Goldak's double ellipsoidal heat source model.

Fillet welds are employed in joining stiffeners in ship structures. Welding residual stresses in fillet welds and their associated redistribution under cyclic loading are poorly understood. distributed in a non-uniform manner. Given the limited guidance in BS 7910 on the assessment of fillet welds and their residual stress redistribution upon mechanical loading, this work employs numerical simulations using Goldak's double ellipsoidal heat source model to predict residual stress response.

Welding simulation involves a two-step thermo-mechanical model. First, a representative thermal analysis using a moving heat source (weld torch) is established. The simulation of arc welding process can be best performed by using Goldak double ellipsoid heat source.

The next task for the thermal analysis requires the calibration of the heat source by means of experimental data which is usually determined from the actual welding of the component of a mock-up. To achieve a better accuracy, the temperature distribution at the weld is compared to the weld pool and the HAZ. A macrograph of the weld metal specimen allows direction determination of bead sizes. Appropriate parameters are then iteratively adapted to match the estimated temperature distributions with the acquired experimental data. The calibration of the heat input in the thermal part of the analysis is often considered a pre-requisite for accurate residual stress and distortion results.

The material properties required for a successful weld residual stress simulation are extensive. Temperature dependent properties for the parent and weld filler materials must be defined from room temperature to well above the melting point of the materials. R6 procedure makes a distinction between 'basic' and 'accurate' analyses: the basic analysis has fewer demanding materials data requirements, reflecting both lower accuracy requirements and the general observation that material properties below about 0.6 Tm have the greatest influence on the final residual stress field.

Once the temperature distribution is determined, it is then used as load input in an elastic-plastic structural analysis to calculate the structural response in terms of residual stresses. The mechanical FE analysis is normally performed as a non-linear static analysis using the transient thermal solution as an applied load. Both simulation parts require temperature dependent material properties.

II. HEAT SOURCE MODELLING

Welding process simulation is implemented in this work to simulate the initial as-welded residual stress distribution on double sided fillet welded T-joint specimen. A thermal elastic-plastic analysis is employed using Goldak's double ellipsoid heat source distribution (Figure 1a) to accurately model the welding process of the T-joint joint specimen. The Goldak's heat distribution replicates the torch movement by following the path defined by the coordinate system. In case of fillet weld joints transformation of coordinates (Figure 1b) is recommended to imulate the weld torch angle of actual welding.

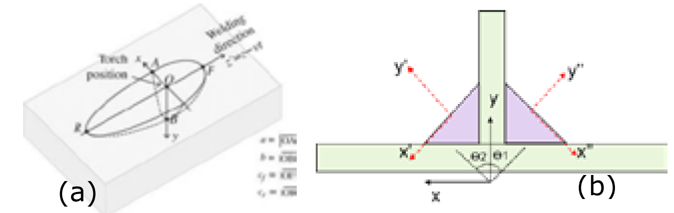

$$q_f(x,y,t) = \frac{6\sqrt{3}\ Qf_f}{abc_f\sqrt[\pi]{\pi}}\ e\left[\frac{-3x^2}{a^2} - \frac{3y^2}{b^2} - \frac{3z^2}{c_f^2}\right]$$ **Equation 1 heat distribution at the front of ellipsoid**

$$q_r(x,y,t) = \frac{6\sqrt{3}\ Qf_r}{abc_r\sqrt[\pi]{\pi}}\ e\left[\frac{-3x^2}{a^2} - \frac{3y^2}{b^2} - \frac{3z^2}{c_r^2}\right]$$ **Equation 2 heat distribution at rear of ellipsoid**

Figure 1: (a) schematic of Goldak's Double ellipsoid heat source; (b) coordinate transformation for fillet weld specimen

As in the present study the welding is performed on both side of the fillet, hence two different heat source parameters are employed, and respective coordinate transformation was achieved by using at an angle of +45° and -45°. A macrograph of the fillet weld is shown in Figure 2.

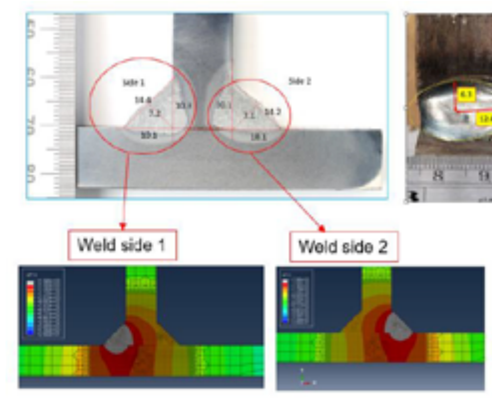

Throat (mm)	Side 1 7.2	Side 2 7.1
a (mm)	8.9	8.9
b (mm)	10.2	10.2
Cf (mm)	7.9	7.9
Cr (mm)	14.6	14.6
Ff (mm)	0.7	0.7
Fr (mm)	1.3	1.3

Figure 2: cross-sectional view of fillet weld specimen used for calibration of Goldak heat source parameters for a 2D model

To validate the 2D weld model a linear heat transfer analysis was conducted, and the shape of the weld bead was compared to the weld cross section macrograph. A 4-node linear heat transfer quadrilateral element is used. Similarly for the 3D model an 8-node linear heat transfer brick is employed. The heat source and the arc movement is deployed in the thermal analysis by a user subroutine DFLUX (compiled in Fortran). In both models the weld metal and base metal is assumed to have same material property. The solidus and liquidus temperature are assumed to be 1450°C and 1500°C respectively. Convection of value 20W/m2K and Radiation with emissivity 0.8 and the Stefan Boltzmann constant 5.67E-8 W/m2K4 is applied as the boundary conditions.

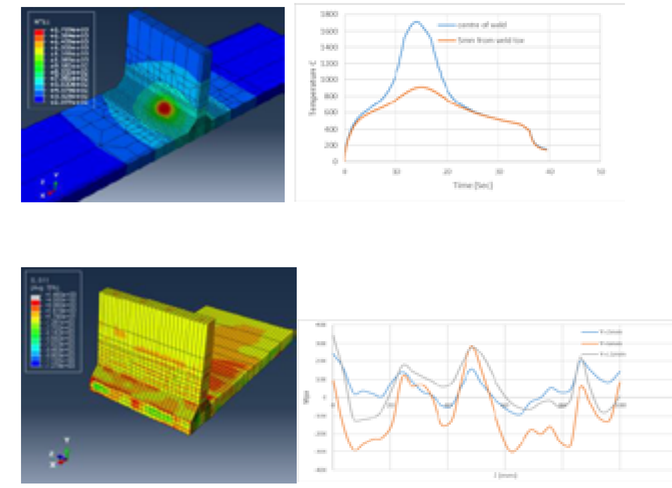

Figure 3: Weld residual stress obtained from the weld model

III. FINDINGS/RESULTS

The Goldak's heat source parameters are determined successfully for the 2D weld geometry. However the same parameters do not lead to satisfactory prediction in a 3D model. This is believed to be caused by the presence of varying depth and width plane between the 2D and 3D models. Further work on 3D weld modelling is going on and the next step would be to calibrate the temperature profile with the temperature data from the weld experiment.

VI. REFERENCES

Goldak, J. A. and Akhlaghi, M. (2005) Computational welding mechanics, Computational Welding Mechanics. doi: 10.1007/b101137

Chujutalli, J. H., Lourenço, M. I. and Estefen, S. F. (2020) 'Experimental-based methodology for the double ellipsoidal heat source parameters in welding simulations', Marine Systems and Ocean Technology, 15(2), pp. 110–123. doi: 10.1007/s40868-020-00074-4.

ACKNOWLEDGEMENT

This research project and the studentship are part of university's strategic collaboration with National Structural Integrity Research centre, based at The Welding Institute. The project is funded by Lloyd's Register Foundation and the research is based in TWI under Coventry University.

Lloyd's Register Foundation helps to protect life and property by supporting engineering-related education, public engagement and the application of research.

Selamawit Abate
Selamawit joined TWI and Brunel University London as a Mechanical and Aerospace Engineering PhD student in 2021. Her research focus is the design improvement of a device based on magnetic flux leakage as one of the most efficient non-destructive testing techniques. The research is funded by Lloyd's Register Foundation and Brunel University London. She received an MSc in Materials Science Exploiting Large-Scale Facilities under the Erasmus Mundus program in France and a BSc in Materials Science and Engineering from Adama Science and Technology University in Ethiopia. In addition, she worked as an academic and research assistant in the School of Mechanical, Chemical and Materials Engineering for a year.

Sensitivity analysis of magnetic circuit components of magnetic flux leakage device for appropriate magnetisation

Owen Rees-Lloyd[1], Dorothee Panggabean[1], Nenad Djordjevic[2], Rade Vignjevic[2]
[1]TWI, [2]Brunel University London
2nd Year of PhD

Keywords: Non-destructive testing (NDT), Magnetic flux leakage (MFL), Magnetic circuit, Oil and gas pipelines, Defect, Finite element modelling (FEM), COMSOL.

I. INTRODUCTION

Ferromagnetic pipelines are used to transport oil and gas. However, they are prone to corrosion [1]. Thus, a number of non-destructive testing (NDT) techniques have been developed to inspect the integrity of the pipelines and predict damage progress. Magnetic flux leakage (MFL) inspection is an NDT technique that can detect both near and far surface defects in ferromagnetic structures [2]. MFL concept is based on inducing a magnetic field in a ferromagnetic pipeline and measuring the magnetic flux, which might be redirected due to an imperfection in the material

MFL consists of a magnetic circuit and sensor. The magnetic circuit is determined by the path followed by the magnetic flux lines. An example of a magnetic circuit containing permanent magnets, a magnet bridge, two pole pieces, lift-offs and an inspection component is shown in Figure 1. The permanent magnet is a source of a magnetic field in the circuit. The magnet bridge is a ferromagnetic material that bridges the two magnet poles. The pole piece is a ferromagnetic material that transfers flux from magnets to the sample. The Lift-off is an air gap. There are two types of lift-offs, a magnetiser lift-off and a sensor lift-off. The magnetiser lift-off is the air gap between the sample and the magnetiser. The sensor lift-off is the air gap between the sensor and the sample. The working principle of MFL is illustrated in Figure 1. When MFL is used on a corrosion-free sample, magnetic flux will be induced in the sample, as shown in Figure 1 (a). However, as shown in Figure 1 (b), magnetic flux leakage will occur when defects are present as the magnetic flux can no longer be contained within the reduced wall thickness.

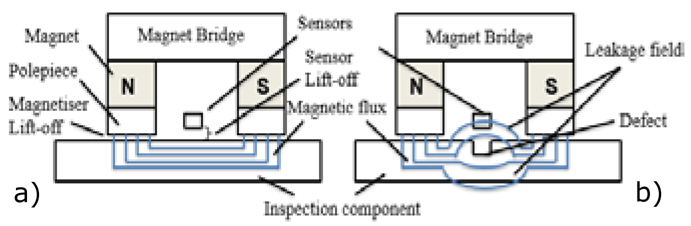

Figure 1, MFL and its working principles of MFL (a) Steel without flaw. (b) Steel with a flaw.

Previous research has considered the effects of a limited number of magnetic circuit parameters. Therefore, this research aims to improve the design of the MFL device by using in-detail sensitivity analysis and optimisation of magnetic circuit parameters for a range of applications of interest to TWI and Lloyd's Register Foundation.

II. METHODOLOGY/APPROACH

A validated methodology is developed using numerical and experimental research. A finite element analysis model constructed within COMSOL Multiphysics is used to design the magnetic circuit. The magnetic circuit consists of permanent magnets, Neodymium iron Boron (NdFeB), and low-carbon steel materials. Analysis of the circuit design and geometry on magnetisation level and defect detection is also investigated. Finally, verification and validation of the numerical results will be done against the experimental data.

III. RESULTS

Magnetisation is a process of making ferromagnetic materials temporarily or permanently magnetic. It is a significant factor in MFL inspection. Sensitivity analysis of magnetic circuit parameters was undertaken to analyse the effect of magnetic circuit parameters on magnetisation level by placing a Hall effect sensor in the middle of the inspection component. Figure 2 shows magnetic flux density norm behaviour in 2D FEA.

The magnet width determines magnetomotive force along the circuit. Thus, Bx increases sharply with increasing magnet width, as shown in Figure 3 (a). In contrast, Bx increases slightly with increasing magnet height, as shown in Figure 3 (b), because increasing the height increases magnetic reluctance.

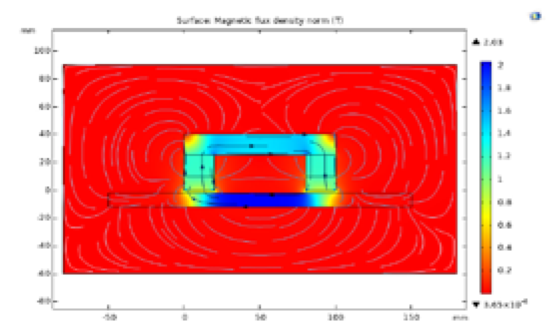

Figure 2, Magnetic flux density behaviour in 2D evaluated with COMSOL.

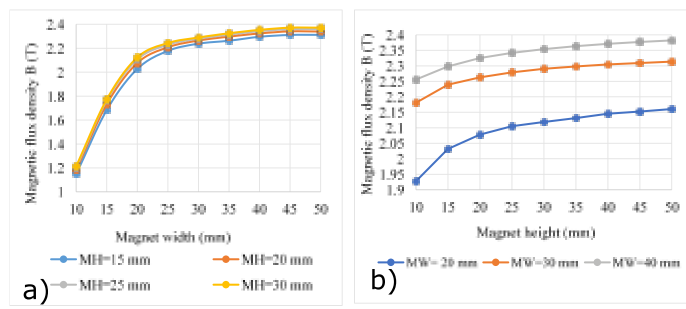

Figure 3, Magnetic flux density vs magnet width (a) and height (b) obtained in 2D FEA.

Magnetic flux density decreases with increasing inspection component thickness and magnetiser lift-off, an air gap between the sample and the rest of the magnetic circuit, as shown in Figure 4, (a) and (b), respectively. While increasing the sample thickness, a bigger magnet is required. Moreover, lift-off causes the distribution of a magnetic field outside the magnetic circuit.

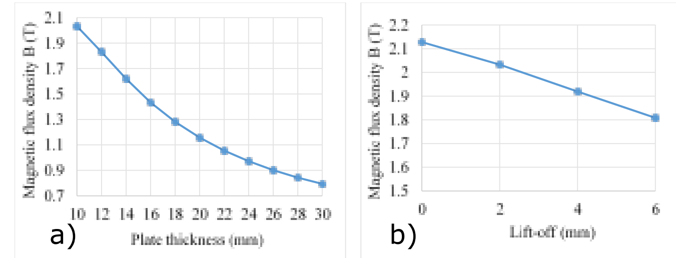

Figure 4, Magnetic flux density vs sample thickness (a) and magnetiser lift-off (b).

IV. CONCLUSIONS

- The circuit parameters' dimensions affect the magnetisation level.
- The magnetisation level increases with increasing magnet width and height.
- Increasing the magnet width affects the magnetisation level more than increasing the height.
- The magnetisation level drops with increasing plate thickness and lift-off.

V. FUTURE PLAN/DIRECTION

- Optimisation of the magnetic circuit design using an optimisation module in COMSOL Multiphysics.
- Analysing machined and actual defects of both near and far-surface of a very narrow rectangular crack and cavity defect (pit) of different dimensions.
- Experimental validation.

ACKNOWLEDGEMENTS

This publication was made possible by the sponsorship and support of Lloyd's Register Foundation and Brunel University London. The work was enabled through, and undertaken at, the National Structural Integrity Research Centre (NSIRC), a postgraduate engineering facility for industry-led research into structural integrity established and managed by TWI through a network of both national and international Universities. Lloyd's Register Foundation helps to protect life and property by supporting engineering-related education, public engagement and the application of research.

REFERENCES

[1] Y. Shi, C. Zhang, R. Li, M. Cai, and G. Jia, "Theory and application of magnetic flux leakage pipeline detection," Sensors (Switzerland), vol. 15, no. 12. MDPI AG, pp. 31036–31055, Dec. 10, 2015. doi: 10.3390/s151229845.
[2] B. Feng, J. Wu, H. Tu, J. Tang, and Y. Kang, "A Review of Magnetic Flux Leakage Nondestructive Testing," Materials, vol. 15, no. 20. MDPI, Oct. 01, 2022. doi: 10.3390/ma15207362.

Soumyadeep Datta

Soumyadeep received his Bachelor's education from National Institute of Technology Durgapur in India with first class (B.Tech.). To pursue his aspirations, he gained an opportunity to study Metallurgical Engineering with specialisation in Materials Science of steels at RWTH Aachen University (M.Sc.), where he graduated with first class. His Master's degree covered application of optimisation algorithms in the metallurgical process of forging, inclusion engineering and compression testing of steels. His research background is mainly in the field of Mechanical Metallurgy. Soumyadeep is currently an NSIRC PhD student of Coventry University and is funded by the Lloyd's Register Foundation and Coventry University. Lloyd's Register Foundation helps to protect life and property by supporting engineering-related education, public engagement and the application of research. His research is focused on the "Establishment of the Sensitivity of Neutrons to Hydrogen in Steels".

Sensitivity of neutrons to hydrogen in steels

Kuveshni Govender[1], Michael Fitzpatrick[2], Mingwen Bai[2]
[1]TWI, [2]Coventry University
2nd Year of PhD

Keywords: Hydrogen diffusion, hydrogen concentration, neutron imaging, sensitivity of neutrons, transmission

I. INTRODUCTION

Cathodic protection (CP) is a commonly used method to protect subsea oil and gas pipelines from electrochemical corrosion. The release of electrons from the sacrificial anode in cathodic protection, in presence of corrosive H^+ environment in seawater, produces atomic hydrogen which is first adsorbed on the surface and thereafter absorbs into the lattice (Truschner, Trautmann, and Mori 2021). Diffusion of hydrogen can embrittle the steel, particularly in the regions of high tensile stress.

An overall relation between the formation and growth of fatigue cracks with the hydrogen contained in the structure is not fully understood. Hydrogenated samples enhance the fatigue crack growth rate significantly (Fassina et al. 2013). A significant reduction in number of cycles to failure is observed for hydrogenated samples (Murakami, Kanezaki, and Mine 2010). Previously only the bulk hydrogen content in steels have been measured and thereafter correlated to the fatigue crack growth rate (Kanezaki et al. 2008). Moreover, investigation of local hydrogen content at corrosion pits, cracks, crevices and tips of cracks have not been carried out in prior research studies. The aim of the current research is the establishment of the relationship between levels of hydrogen and damage modes.

Neutron diffraction is a non–destructive testing method which has high penetration compared to X-rays and electrons, as well as generates a significant difference in contrast for hydrogen with iron. The cross section of neutrons interacting with hydrogen atom is approximately 7.5 times the cross section of neutrons interacting with iron atom (Griesche et al. 2015).

The neutron imaging technique offers the advantage of examination of large samples in both ambient and corrosive environments. To study the location and intensity of transmitted radiation through the sample, the use of a detector is made which records the contrast between the sample and surroundings as well as in different regions of the sample. The neutron transmission is essential for establishment of sensitivity of hydrogen to neutrons. The design of assets in oil and gas industry, critical assessment of largest tolerable flaw sizes in pipelines, and life extension of subsea structures in service are dependent on the outcome of this project.

II. METHODOLOGY

A. Sample Preparation

Identical samples with dimensions of 100x20x10 mm were prepared with different grades [X65 and 316] of steel. A sample 316 with dimension 100x20x10 mm was used for reference in neutron imaging. Samples supplied by the Test House [TTH], underwent EDM notching and were polished to reduce surface roughness to ~1 µm. The notched samples, as shown in Figure 1 were subjected to fatigue pre-cracking using a constant stress intensity factor range of 400N/mm$^{3/2}$, load ratio 0.1 and frequency of 8Hz. The pre-crack length is 1mm from the notch tip. Post pre-cracking, samples were electrochemically charged in a 3.5% NaCl sodium under cathodic protection.

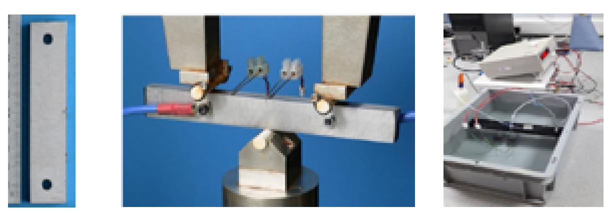

[a] [b] [c]
Figure 1: Samples [a] pre-cracking [b] charging [c]

B. Hydrogen Charging and Bulk Estimation

A conventional three electrode cell which consists of a working electrode (steel sample), Pt counter electrode and a reference electrode of Ag/AgCl, connected through a salt bridge to the electrolyte, was used for conducting underwater H charging at RT using 3.5% NaCl electrolyte. Potential was set at -1.1V, and charging time was varied to understand hydrogen concentration variation, as in Figure 2. H charging at 300°C and 100bar was also performed. The bulk diffusible H was measured for the entire sample using area under the diffusion rate against time curve at 400°C in G4-Phoenix CGHE machine at TWI Ltd. and bulk trapped H was measured for the crack [in a 5mmx20mmx10mm region] at 900°C, as in Figure 2.

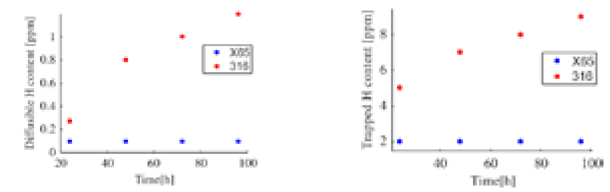

[a] [b]
Figure 2: Diffusible H [a] Trapped H [b]

C. Neutron Imaging through Radiography

Higher hydrogen concentration was obtained using 316 steel grade. The 316 samples were charged for long duration [673h] at 40°C. These samples were dipped in liquid N_2 to prevent H desorption and subjected to neutron radiography at IMAT [ISIS-RAL]. A polychromatic neutron beam was projected on the sample set [reference and hydrogenated sample placed together] with a tube length of 56.5m, using two different detectors [MCP (detector size 28mmx28mm) and CMOS (scintillator based detector)], with sample placed close to the detector (to avoid scattering effect). Spatial resolution was 100µm, and a fine binning of 2000 points were considered for analysis.

III. FINDINGS/RESULTS

Figure 3 shows the variation of contrast at the edges for an electrochemically charged and cracked sample. The dip in grey value is attributed to refraction resulting in edge enhancement.

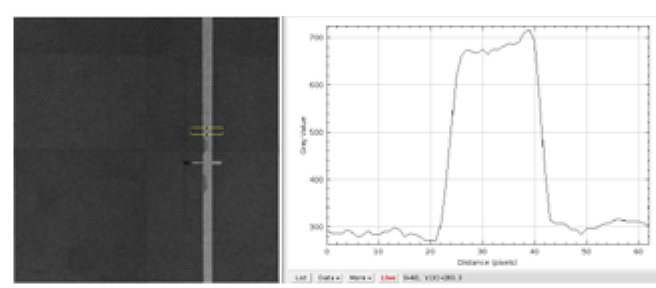

Figure 3: Edge enhancement shown during imaging

The possibility of moisture condensation is also not ruled out. Sudden dip in contrast in Figure 4 is possible due to condensation.

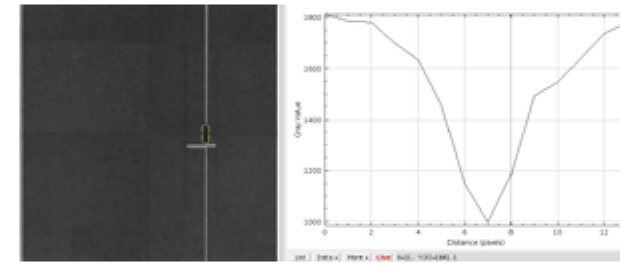

Figure 4: Possible condensation during imaging

IV. DISCUSSION/CONCLUSIONS

- Distributed change in transmission observed, analysis requires higher H concentration for a clearer picture.
- Edge enhancement and moisture formation results in change of contrast. Calibration should consider these effects for accurate estimation.

V. FUTURE PLAN/DIRECTION

- To increase hydrogen content, evaluate change in crack growth rate with hydrogen content, and calibrate transmission with hydrogen contrast.

REFERENCES

Fassina, P., Brunella, M. F., Lazzari, L., Re, G., Vergani, L., and Sciuccati, A. (2013) 'Effect of Hydrogen and Low Temperature on Fatigue Crack Growth of Pipeline Steels'. *Engineering Fracture Mechanics* 103, 10-25

Griesche, A., Dabah, E., Kannengiesser, T., Hilger, A., Kardjilov, N., Manke, I., and Schillinger, B. (2015) 'Measuring Hydrogen Distributions in Iron and Steel using Neutrons'. *Physics Procedia* 69, 445-450

Kanezaki, T., Narazaki, C., Mine, Y., Matsuoka, S., and Murakami, Y. (2008) 'Effects of Hydrogen on Fatigue Crack Growth Behavior of Austenitic Stainless Steels'. *International Journal of Hydrogen Energy* 33 (10), 2604-2619

Murakami, Y., Kanezaki, T., and Mine, Y. (2010) 'Hydrogen Effect Against Hydrogen Embrittlement'. *Metallurgical and Materials Transactions A* 41, 2548-2562

Truschner, M., Trautmann, A., and Mori, G. (2021) 'The Basics of Hydrogen Uptake in Iron and Steel'. *BHM Berg- Und Hüttenmännische Monatshefte* 166 (9), 443-449

ACKNOWLEDGEMENTS

The aforesaid publication was possible only due to the sponsorship and support of the Lloyd's Register Foundation as the funding source of this project and Coventry University. The aforesaid works were undertaken at the National Structural Integrity Research Centre (NSIRC), a postgraduate engineering facility for industry-led research into structural integrity established and managed by TWI through a network of both national and international Universities. At the UKRI ISIS facility located at Rutherford Appleton Laboratory Oxford, the neutron imaging was performed using the beamline IMAT.

Man Chi Cheung

Pursued an MSc in Oil and Gas Engineering at Brunel University London with a research focusing on the structural integrity of composite structures, Man Chi continues her career development and research with Brunel University London on designing a novel composite-to-metal joint for the application in naval vessels by adopting an existing stud forming technology invented in TWI. The specified objectives of her Ph.D. project are primarily driven by an extensive simulation programme, which will be verified and validated against experimental results. This research is funded by TWI's Core Research Programme. The work was enabled through, and undertaken at, the National Structural Integrity Research Centre (NSIRC), a postgraduate engineering facility for industry-led research into structural integrity.

Composite-to-metal joining for naval vessels

Dr Chris Worrall[1], Dr Nenad Djordjevic [2], Dr Mihalis Kazilas[2]
[1]TWI, [2] Brunel University London
3rd Year of PhD

Keywords: dissimilar material joints; refill friction stir spot welding (RFSSW); resin infusion; finite element modelling; failure mechanism analysis

I. INTRODUCTION

To reduce the weight of naval vessels, it has long been a goal to employ composite materials for their superstructures. However, joining the composite top to the metallic bottom is challenging. A solution is to produce the composite containing a metallic edge at the bottom so that it can easily be welded to the metal deck using conventional shipyard techniques, such as arc welding. Adhesive bonding and mechanical fastening are the two typical methods to join composite to metal. However, adhesive bonding has poor resistance to peel loads and it is sensitive to surface preparation and susceptible to environmental degradation. To join composites by mechanical fastening, holes have to be drilled for fastener installation, which cuts the load-carrying fibres and thus reduces its strength. In addition, fasteners add weight to the structures. To meet the industrial needs and overcome the shortcomings, this project develops a composite-to-metal joint as shown in Figure 1.

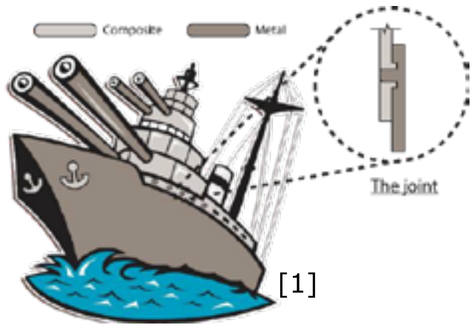

Figure 1. Concept of the composite-to-metal joint.

II. CONCEPTUAL DESIGN OF THE JOINT

The joint, as illustrated in Figure 2, is made of aluminium alloy 6082 and plain woven E-glass fabric reinforced epoxy. To produce the joint, a stud is machined out of the metal adherend, then embedded into the composite adherend before resin infusion and curing.

Figure 2. Design concept of the metal stud joint.

To produce the metal stud, a sleeve plunges into the plate with high speed rotation as shown in Figure 3. The frictional heat generated softens and restructures the metal plate to form studs, which are embedded to the composite.

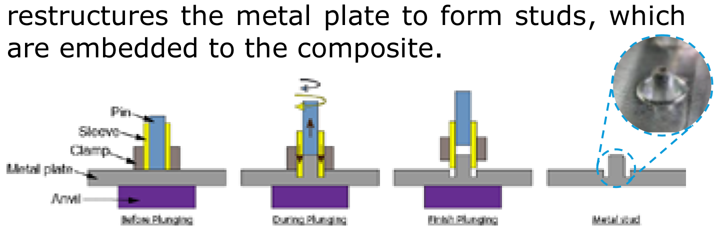

Figure 3. Metal stud manufacturing process.

Figure 4 shows how the composite adherend is assembled to the metallic adherent to form a joint. The dry fabric is first placed onto the metal stud so that the woven fibres of the fabric are not damaged, but are shifted around the stud. Resin is then infused into the system after multiple plies of fabric are put in place.

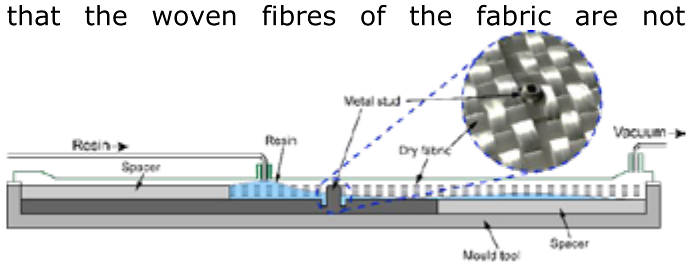

Figure 4. Resin infusion for joint manufacturing.

Apart from no additional weight and maintained fibre continuity, the joint provides smooth surfaces without screw heads or nuts, and is expected to potentially improve the reliability of conventional bonded or bolted joints.

III. EXPERIMENT APPROACH

To access the strength of the joint, the first set of the single-lap shear tests is carried out. Two groups of specimens were tested: one with a metal stud in the centre of the overlap area and one without as shown in Figure 5.

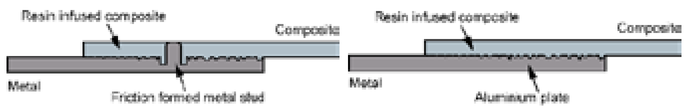

Figure 5. Joint specimens with (left) and without (right) metal stud for single-lap shear tests.

Force-displacement curves from the single-lap shear tests are shown in Figure 6.

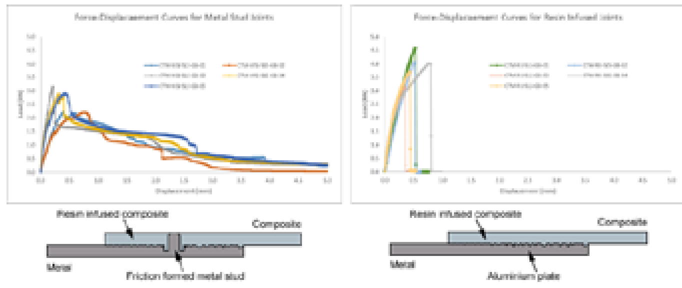

Figure 6. Force-displacement curves for joints with (right) and without (left) metal stud.

Comparison of the curves obtained with the two joints is illustrated in Figure 7. Although the joint without metal stud achieves higher joint strength, the joint with metal stud absorbs more energy, which may be beneficial in terms of damage tolerance of the joint failure. The reduction of the joint strength with the presence of a metal stud is due to the reduction of the overlapped area.

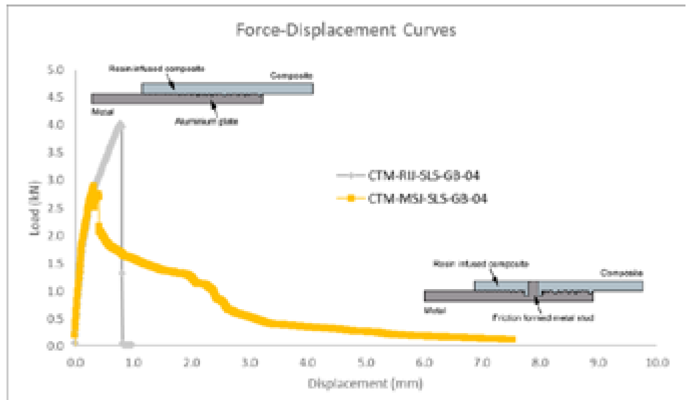

Figure 7. Comparison of force-displacement curves from composite-metal joints with and without metal stud.

IV. SIMULATION APPROACH

To understand the failure mechanism, a numerical model for the joint with a metal stud in the centre of the overlapped area is developed as shown in Figure 8. The simulation results show that the joint first failed at debonding, followed by compression damages caused by the bending of the metal stud.

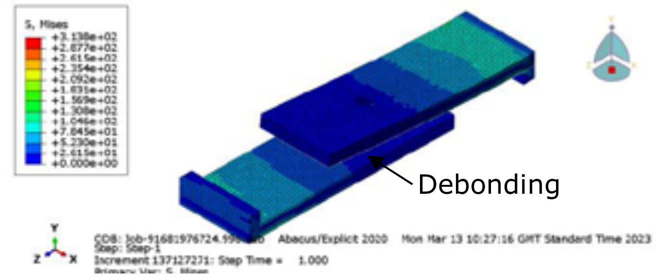

Figure 8. Debonding is the first failure for single-lap shear test.

The region experienced fibre compressive damage is shown in Figure 9. Matrix compressive damage is also found in a similar location.

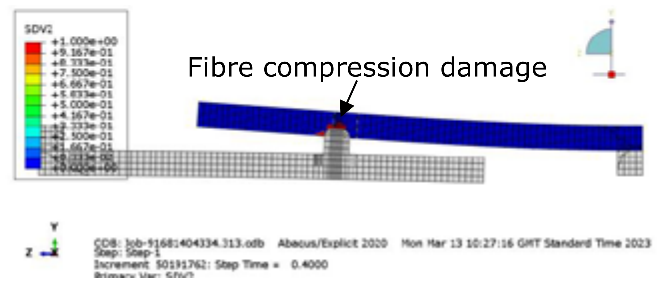

Figure 9. Region for fibre compression damage.

V. CONCLUSIONS AND FUTURE PLAN

Metal studs machined from the metallic adherend can be used in a composite to metal joint without adding any weight to the structure. The first experimental results shown that the stud improves energy absorption capacity by 2.3 times.

To further compare performance of the new joint and potentially improve its strength, by adding an adhesive layer to the metal-composite interface, a new set of experiments will be carried out, with the joint configurations illustrated in Figure 10.

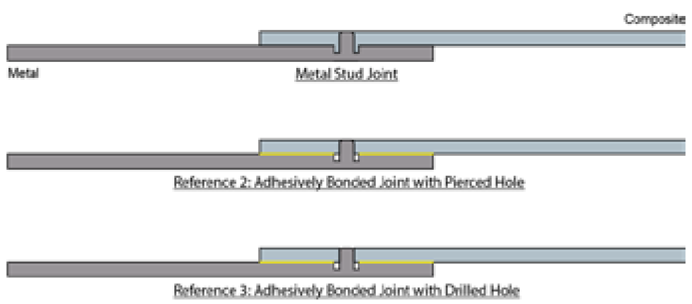

Figure 10. Joint configurations to be studied.

REFERENCES

[1] "battleship game logo," Clip Art Library, 2023. [Online]. Available: http://clipart-library.com/clip-art/battleship-silhouette-8.htm.

Haolin Fei

Haolin Fei is a third-year PhD candidate in Engineering at Lancaster University. He received his Bachelor of Engineering in Electronic Information Engineering from the University of Electronic Science and Technology of China and his first-class honours Bachelor of Engineering degree in Electronics and Electrical Engineering from the University of Glasgow. His research is funded by the Lloyd's Register Foundation and focuses on the application of robotics and artificial intelligence in industrial processes. Haolin's research interests include deep learning, computer vision, and bio-inspired algorithms and frameworks for robotics. He is passionate about advancing these areas of research and hopes to make meaningful contributions to the academic community through his work.

Composite-to-metal joining for naval vessels

Darren Williams[1], Ziwei Wang[2], Andrew Kennedy[2]
[1]TWI, [2]Lancaster University
3rd Year of PhD

Keywords: Collaborative Robotics, Brazing Process, Human-Robot Interaction, Deep Reinforcement Learning

I. INTRODUCTION

Brazing is a widely used process in the manufacturing industry, where two or more metal parts are joined by heating them to a temperature above 800°C and using a filler metal [1]. It is a complex and demanding process that requires a high level of skill and expertise, and the shortage of skilled brazing workers poses a significant challenge for the industry. The quality of brazed joints depends on various factors, including the operator's skill, temperature control, and filler metal flow rate [2]. In addition, the process involves working with high temperatures, hazardous fumes, and potentially dangerous equipment, which increases the risk of accidents and injuries [3].

To address these challenges, there has been a growing interest in integrating collaborative robots, also known as cobots, into the brazing process [4-7]. Cobots are designed to work alongside human operators and can perform repetitive and physically demanding tasks, enhance precision and accuracy, and improve safety by reducing the risk of accidents and injuries [8].

This paper proposes a novel human-robot collaborative framework for the brazing process that employs trajectory regression and deep reinforcement learning to enhance the accuracy, efficiency and productivity of the process. The proposed framework involves the use of a cobot that can assist the operator in the brazing process by taking over some of the more repetitive or dangerous tasks, such as controlling the temperature and filler metal flow rate. The cobot's actions are guided by a reinforcement learning algorithm that uses feedback from the operator to improve its performance over time. Additionally, the proposed framework utilises trajectory regression to predict the optimal path and trajectory of the brazing tool, further improving the quality and accuracy of the brazing process.

The proposed human-robot collaborative framework has the potential to revolutionise the brazing process, reducing the reliance on skilled labour and improving the safety and quality of brazed joints. This research is highly relevant to the manufacturing industry, where the integration of cobots has become an increasingly popular trend in recent years. The proposed framework can serve as a starting point for future research in the field of collaborative robotics, and could potentially be applied to other industrial processes beyond brazing.

II. DESIGN/METHODOLOGY/APPROACH

The proposed human-robot collaborative framework for the brazing process involves several steps. Firstly, the workpiece is tagged with a QR code, which the robot reads to identify the workpiece and determine whether the process requires human intervention. If human intervention is not required, the robot autonomously performs the brazing process according to the instructions or previous experience. However, if the process requires human intervention, the operator performs the brazing task, and the robot records the trajectory data. Subsequently, the trajectory regression algorithm generates a trajectory for the robot to replicate the operator's actions. This approach enables the robot to learn from the operator's actions and perform the brazing process with greater precision.

Secondly, the proposed framework includes a reaching algorithm which can be regarded as a supernumerary limb that includes a reaching process. The robot employs RGB images and a deep reinforcement learning algorithm for unseen object reaching. This approach allows the robot to adapt to scenarios with unknown and variable target object positions, thus enhancing the flexibility of the brazing process. The proposed framework does not require a depth sensor, which reduces the hardware cost and simplifies the implementation of the system.

III. FINDINGS/RESULTS

The proposed framework was tested in a simplified brazing scenario, and the results demonstrate that the framework was able to effectively adapt to different workpieces and scenarios while significantly reducing the likelihood of errors and inconsistencies caused by human factors. Overall, the proposed framework was found to be a highly reliable and efficient solution to the current shortage of skilled brazing workers in the industry.

IV. DISCUSSION/CONCLUSIONS

The proposed human-robot collaborative framework for the brazing process presents a promising solution to the shortage of skilled brazing workers in the industry. By leveraging state-of-the-art technologies in computer vision, AI and robotics, the framework paves the way for the development of advanced manufacturing systems that can operate in dynamic and complex environments. Moreover, the application enables the robot to learn and adapt to different scenarios, thereby can also be applied to other industrial process for improving the quality and flexibility.

V. FUTURE PLAN/DIRECTION

Future research will focus on further improving the performance of the trajectory regression algorithm and the deep reinforcement learning models employed in the framework. Additionally, the framework will be extended to other manufacturing tasks, such as welding and soldering, to enhance the efficiency, productivity, and safety of the manufacturing industry. The proposed framework provides a foundation for the development of advanced manufacturing systems that can adapt to the dynamic and complex environment of modern manufacturing.

The proposed framework's adaptability to different scenarios and workpieces makes it a versatile solution that can be applied across a broad range of industries. The framework's successful application to the brazing process provides a strong foundation for the development of advanced manufacturing systems that can adapt to the dynamic and complex environment of modern manufacturing. With the continued development and refinement of such systems, the manufacturing industry can overcome current challenges and pave the way for a more productive and efficient future.

REFERENCES

[1] American Welding Society C3 Committee on Brazing and Soldering. Brazing handbook. Miami: American Welding Society, 2011.
[2] Schwartz MM. Brazing. ASM international; 2003.
[3] Sekulić DP, editor. Advances in brazing: science, technology and applications. Elsevier; 2013 Mar 4.
[4] Djuric AM, Urbanic RJ, Rickli JL. A framework for collaborative robot (CoBot) integration in advanced manufacturing systems. SAE International Journal of Materials and Manufacturing. 2016 May 1;9(2):457-64.
[5] Bragança S, Costa E, Castellucci I, Arezes PM. A brief overview of the use of collaborative robots in industry 4.0: human role and safety. Occupational and environmental safety and health. 2019 Feb 28:641-50.
[6] El Makrini I, Elprama SA, Van den Bergh J, Vanderborght B, Knevels AJ, Jewell CI, Stals F, De Coppel G, Ravyse I, Potargent J, Berte J. Working with walt: How a cobot was developed and inserted on an auto assembly line. IEEE Robotics & Automation Magazine. 2018 May 16;25(2):51-8
[7] Peshkin MA, Colgate JE, Wannasuphoprasit W, Moore CA, Gillespie RB, Akella P. Cobot architecture. IEEE Transactions on Robotics and Automation. 2001 Aug;17(4):377-90.
[8] El Zaatari S, Marei M, Li W, Usman Z. Cobot programming for collaborative industrial tasks: An overview. Robotics and Autonomous Systems. 2019 Jun 1;116:162-80.

VI. ACKNOWLEDGEMENTS

This publication was made possible by the sponsorship and support of Lloyd's Register Foundation. The work was enabled through, and undertaken at, the National Structural Integrity Research Centre (NSIRC), a postgraduate engineering facility for industry-led research into structural integrity established and managed by TWI through a network of both national and international Universities. Lloyd's Register Foundation helps to protect life and property by supporting engineering-related education, public engagement and the application of research.

Kartikey Mathur

Funded by Lloyd's Register Foundation (LRF), Kartikey started his PhD at NSIRC in January 2021. With a Bachelor's Degree in Mechantronics Engineering and a Master's in Naval Architecture & Ocean Engineering, he has a diverse experience in the field of automation. His PhD project focuses on on-line monitoring of Friction Stir Welding and aims to induce more confidence in the process adressing major knowledge gaps in the domain of on-line defect detection for FSW.

Weld quality assessment of FSW joints by continuous acoustic emission monitoring

Stephen Cater[1], Andrew Kennedy[2], Xia Min[2]

[1] TWI , [2] Lancaster University
3rd Year of PhD

Keywords: Friction Stir Welding, FSW, Acoustic Emission, AE, CNN

I. INTRODUCTION

The Friction Stir Welding (FSW) process has been adopted by manufacturers due to its stability against external factors and its ability to weld dissimilar metals. (FSW) has seen a vast expansion in the past decade. Past research has proven that online control of welding parameters has the potential to improve weld quality[1][2]. Force and position control for FSW are the two widely used control methods. Forces in three directions and advancing & retreating side for FSW is illustrated in Fig-1. The present sensing and control methodology is subjective to the type of defects. A multi-sensory approach has been discussed to address the limitation of the current monitoring methods and has more confidence in the process. The project aims to use Artificial Intelligence (AI) supported by force & acoustic emission (AE) monitoring for the development of classification and control methods. At the current stage in the project timeline, forces in the axial direction and lateral direction along with acoustic emission of the process are used for the development of a weld classification system. The completion of the project would yield a deep learning-based weld quality prediction and control system.

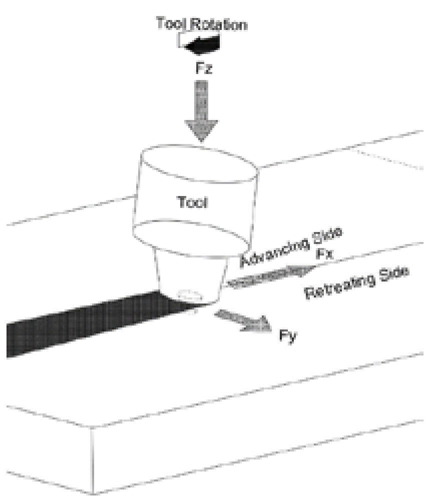

Figure 1 - Forces in three directions and advancing and retreating side of the weld

II. DESIGN/METHODOLOGY/APPROACH

To achieve the aim of the project the methodology of the project could be explained in three, process monitoring, data processing method and implementation of Convolutional Neural Networks (CNN) for classification. The collected AE data can be plotted as spectrograms and co-related with the affect of induced flaws/defects in the weld. With data widening method, the volume for the training data is increased. The CNN model is optimised to achieve the best accuracy. The process of weld classification can be explained with Fig-2.

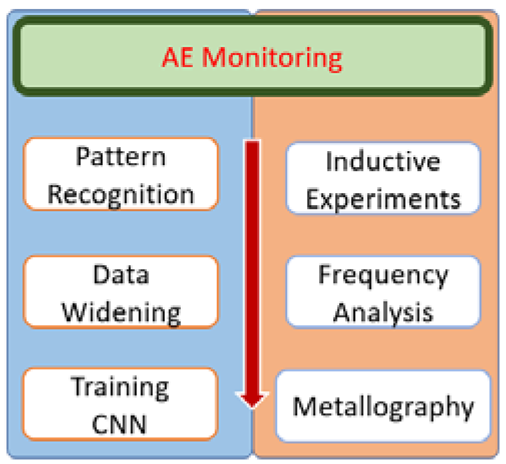

Figure 2 - Research methodology

III. FINDINGS/RESULTS

Addressing the knowledge gap present in the domain of AE-based monitoring, initial trials were focused on correlating force data with the variation in AE during welding. A good correlation between both parameters was observed as shown in Fig-3. The amplitude of the AE signal has also been related to the volume of plasticized material.

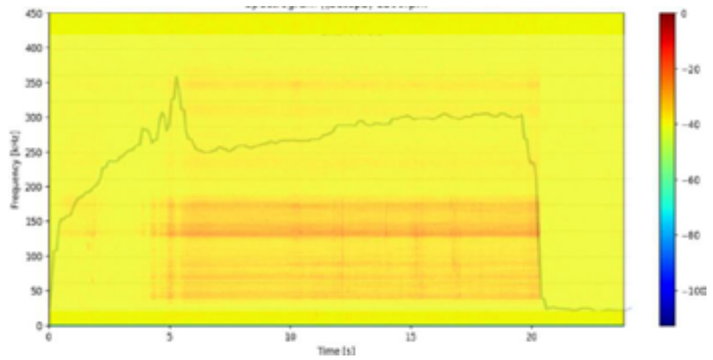

Figure 3 - Spectrogram of the AE data with axial force plotted in the background

The ability of continuous AE monitoring for defect/flaw detection can be defined in four points.

- Ability to detect material flow disruption
- Ensuring shoulder consisting shoulder engagement.
- Detecting the presence of a lack of penetration
- Ability to detect sub-surface cavity/channel defects in the weld. (Shown in Fig-4)

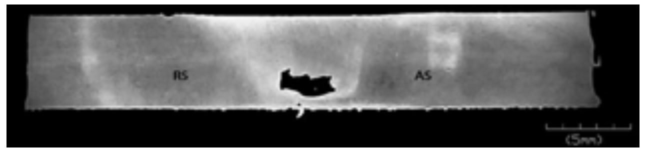

Figure 4 - Sub-surface void for colder welds with labeled Advancing Side(AS) & Retreating Side (RS)

To develop an online weld classification system, CNN models were used (i.e,-VGG16, Resnet-50 & Inception model). Each of the models has different block architecture and the accuracy to time cost was also analysed. The hybrid architecture utilising mel-spectrogram & spectrogram is illustrated in the Fig-5.

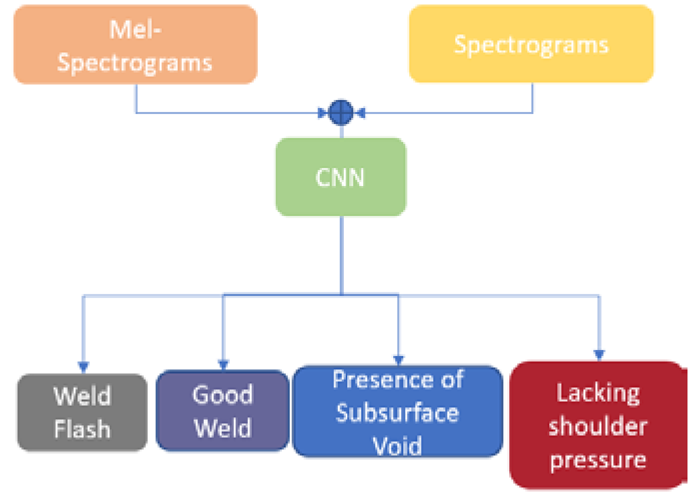

Figure 5 - Hybrid mel-spectrogram & spectrogram architecture

IV. DISCUSSION/CONCLUSIONS

Based on the experimental data collected, the continuous emission monitoring method was successful in detecting the induced flaws and defects. Spectrograms and mel-spectrograms indicated variation in the bandwidth frequency and material flow around the tool was co-related. Training and testing of hybrid mel-spectrogram & spectrogram Convolutional Neural Network (CNN) yielded 92% accuracy for the Inception inspired network.

V. FUTURE PLAN/DIRECTION

The experiments were performed on AA6082 & AA5083, and the results were transferable between materials. Future work can be extended by understanding the AE signals for FSW of dissimilar and harder metals. The possibility of co-relating the AE signal with the void size is also highlighted which can be extended to different materials.

VI. ACKNOWLEDGEMENT

This publication was made possible by the sponsorship and support of Lloyd's Register Foundation. Lloyd’s Register Foundation helps to protect life and property by supporting engineering-related education, public engagement and the application of research. The work was enabled through, and undertaken at, the National Structural Integrity Research Centre (NSIRC), a postgraduate engineering facility for industry-led research into structural integrity established and managed by TWI through a network of both national and international Universities.

REFERENCES

[1] A. Baraka, G. Panoutsos, and S. Cater, “A real-time quality monitoring framework for steel friction stir welding using computational intelligence,” J. Manuf. Process.

[2] D. Ambrosio et al., “On the potential applications of acoustic emission in friction stir welding,” J. Manuf. Process.

Antonios Porichis

Antonios received his MSc-equivalent 5-year Diploma of Engineering in 2012 from the Electrical and Computer Engineering School of the National Technical University of Athens. His Diploma Thesis on Modelling and Evaluation of Laparoscopic Surgical Skill received the Thomaidion Award as the best Diploma Thesis of the same year. From 2013 till 2020 he has worked as a Robotics and Machine Learning engineer taking up positions of Team Manager and Technical Director. Throughout this period he has successfully seen through 6 EU-funded projects involving advanced robotic systems. In April 2021 Antonis joined the University of Essex and NSIRC as a PhD student under the guidance and supervision of Dr. Vishwanathan Mohan and Dr. Panagiotis Chatzakos. His research is sponsored by Lloyd's Register Foundation and focuses on the development of Learning by Demonstration Algorithms for human-to-robot skill transfer that will enable automation of complex tasks.

Learning by demonstration for learning complex manipulation strategies directly from pixels

Panagiotis Chatzakos[1,2], Vishwanathan Mohan[2]
[1]TWI, [2]University of Essex
2nd Year of PhD

Keywords: Visual Imitation Learning, Learning by Demonstration, Complex Manipulation

I. INTRODUCTION

Imitation Learning (IL) techniques can enable robotic agents to learn to perform tasks directly from expert demonstrations [1] without requiring explicit control strategy design. This opens up a huge array of applications where human operators are still required to be involved even though the tasks performed are extremely tedious, low-value and with significant health & safety risks.

Most of the research work around IL, however, is mainly focusing on tasks and agents that respect one or more of the following assumptions: (i) existence of a high number of expert demonstrations or capability to perform lots of iterations to learn the task [1], [2], (ii) that access to the full state of the task is available [3], (iii) that the task can be accomplished purely by considering kinematic rather than the dynamic aspects of the environment [4].

In this work, we implement an IL method for use in a simulated version of a complex task, namely outrooting a fresh mushroom through a combination of motions with a rigid or a soft gripper.

II. METHODOLOGY

Our IL Architecture comprises two main components; a Representation Learning (RepL) module that allows for the high-dimensional input to be cast into a latent space to obtain a low dimensional embedding, and the Behavioural Cloning (BC) module which predicts the next action given the embedding of the current observation.

We use two different datasets to train our models. The first dataset $D_r = \{T_1^r \dots T_N^r\}$ is a collection of N random trajectories. These are created by sampling random actions by rolling forward a Ornstein–Uhlenbeck process. The second dataset, $D_e = \{T_1^e \dots T_M^e\}$ contains M expert demonstrations, driven by a precise rule-based policy that has direct access to the location and orientation of the target, i.e. the mushroom to be picked and the proprioception measurements of the gripper. Each trajectory $T_i = \{(o_k, a_k)\},\ k = 1 \dots K_i$ is a sequence of observation-action pairs as is the case in a standard IL setting.

The RepL module is implemented as a Variational Autoencoder (VAE). The VAE's encoder, $g(o)$, receives and observation o and outputs two vectors, $g^\mu(o)$ and $g^\sigma(o)$ which are treated as the mean and the diagonal covariance matrix of normal distribution. $g^\mu(o)$ is considered an embedding of o in a latent space captured by the VAE. The decoding step requires sampling the normal distribution and then running the sample through the decoder which produces a reconstruction of the original input $\tilde{o}$. The model loss for each observation sample is defined as:

$$l_{VAE}(o) = (o - \tilde{o})^2 + D_{KL}\left(N\left(g^\mu(o), g^\sigma(o)\right), N(0, I)\right)$$

where D_{KL} is the Kullback – Leibler divergence. The overall model is trained by minimizing the mean of the above loss over the entire dataset.

The BC module comprises a Multi-layer Perceptron that receives as input the embedding $u = g^\mu(o)$ and outputs an action prediction $\tilde{a}$. This model is trained to minimise the Mean Squared Error loss. In the case of the soft gripper, force measurements are normalised and concatenated at the end of the embedding.

The model training proceeds in three steps. Firstly, the RepL module is trained on a dataset of random trajectories. Then, a second training stage of the RepL module takes place. This time it is trained with expert trajectories. Finally, the RepL and BC modules are trained jointly on the expert data. This means that the gradients from the L_{BC} loss flow back to the encoder, updating the weights of $g^\mu(o)$. This staged training approach keeps a balance in allocating the representational power of the RepL module to the information contained in the images that is meaningful to predict the actions.

For experiments, we rely on a custom simulation framework modelling the mushroom and gripper dynamics. The simulation is built on top of the PyBullet multibody dynamics physics engine.

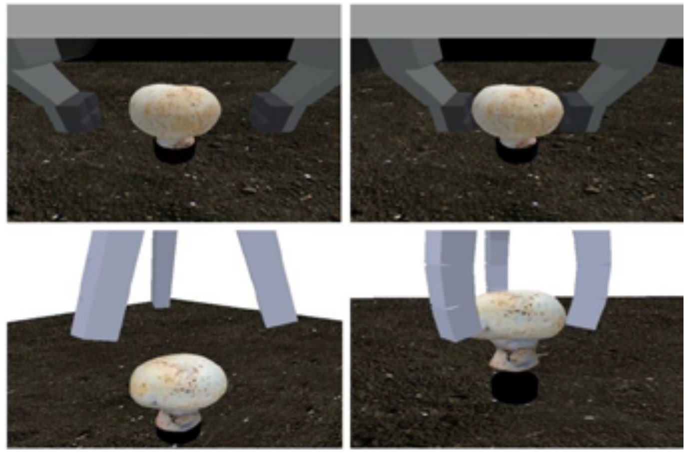

Figure 1 Successful episode rollout snapshots by the trained agents with a rigid and a soft gripper

III. RESULTS

We have conducted experiments in both partially and fully randomised versions of the environment. In the partially randomised version, the size of the mushroom as well as the extrinsic and intrinsic parameters of the camera do not change across episodes. In contrast, in the fully randomised version of the environment we apply variations to the extrinsic parameters of the camera, namely its yaw and pitch angle as well as its distance relative to the gripper as well as to the intrinsic 2D coordinate frame centre. We specifically apply a randomness factor of ±5% across each of these parameters compared to the nominal values. We also vary the size of the mushroom by ±10%.

Furthermore, we test our approach with two different types of images as observations. In the first case we used grayscale images as while in the second case we use artificially noise-corrupted depth maps environment after artificial noise has been added to the depth map. Table 1 summarises the results across all different tests. Success rates were measured on 50 different episode rollouts.

Table 1 Success rates for different variations

Approach	Gripper	Rand.	Success
Expert Only	Rigid	Partial	90%
Random + Expert	Rigid	Partial	96%
Expert Only	Rigid	Full	58%
Random + Expert	Rigid	Full	78%
Random + Expert	Soft	Partial	64%

IV. DISCUSSION

As seen above, our approach successfully reproduces the mushroom harvesting sequence >90% of the time in the partially randomised environments. Pre-training on random trajectories can sustain a 78% success rate even in the case of significant camera perturbation and mushroom size variation, where pure training on expert demos reaches 58%. The approach also handles multi-modal input achieving 64% success on the soft gripper case.

V. FUTURE PLAN

We plan to extend this work by testing the approach on a real robot and physical mushroom mock-ups. In this way we will evaluate the transferability of the approach from simulation to reality.

ACKNOWLEDGMENTS

This publication was made possible by the sponsorship and support of Lloyd's Register Foundation. The work was enabled through, and undertaken at, the National Structural Integrity Research Centre (NSIRC), a postgraduate engineering facility for industry-led research into structural integrity, established and managed by TWI Ltd. through a network of both national and international universities.

REFERENCES

[1] Ho, J., & Ermon, S. (2016). Generative adversarial imitation learning. Advances in neural information processing systems, 29.

[2] Arora, Saurabh, and Prashant Doshi. "A survey of inverse reinforcement learning: Challenges, methods and progress." Artificial Intelligence 297 (2021): 103500.

[3] Torabi, F., Warnell, G., & Stone, P. (2018). Behavioural cloning from observation. arXiv preprint arXiv:1805.01954.

[4] Zakka, K., Zeng, A., Florence, P., Tompson, J., Bohg, J., & Dwibedi, D. (2022, January). Xirl: Cross-embodiment inverse reinforcement learning. In Conference on Robot Learning (pp. 537-546). PMLR

Konstantinos Vasios

Dipl.-Ing Electrical & Computer Engineer (NTUA GR), specialized in robotics & automation, experienced in the development of control software in the automotive and robotics. Currently a PhD Candidate at the University of Essex trying to bring machine intelligence a step closer to the real-world.

This publication was made possible by the sponsorship and support of Lloyd's Register Foundation (LRF). The work was enabled through, and undertaken at, the National Structural Integrity Research Centre (NSIRC), a postgraduate engineering facility for industry-led research into structural integrity established and managed by TWI through a network of both national and international Universities. Lloyd's Register Foundation helps to protect life and property by supporting engineering-related education, public engagement and the application of research.

Bridging the simulation to reality gap in robotics

Dr. Panos Chatzakos[1], Dr. Mohan Vishwanathan[2], Dr. Jarchi Delaram[2] ,
[1]TWI, [2]University of Essex
2nd Year of PhD

Keywords: sim2real; simulation; robotics; mushroom-harvesting; soft-gripper; soft-robotics; reinforcement-learning;

I. INTRODUCTION

Training, evaluating, and deploying AI agents directly into the real world is most often prohibited by severe time, cost, availability, and safety constraints. Modelling and Simulation are therefore instrumental for the design of AI agents with interesting behavioural characteristics, within the realm of Machine & Reinforcement Learning. We test the efficacy of our approaches against a specific and still practically unsolved manipulation problem, that of robotic mushroom harvesting with a soft robotic gripper. We start with the design of a simulation environment for this specific manipulation task and we proceed with an exploration of sim2real techniques for our real-world setup. We propose a novel control pipeline that encapsulates the simulation, not only as a training platform but also as a live, in-situ, abstraction layer.

II. DESIGN/METHODOLOGY/APPROACH

With the design of the simulation framework for mushroom harvesting immediately two well-known problems arise. Firstly, the complexity and intricacies of the contact dynamics are usually not captured by the commonly utilized rigid multibody physics engines for robotics, rendering a robust sim2real transfer unlikely. Secondly, capturing the behaviour of materials with deformable structures and respective failure modes is a hard problem that is usually framed within analytical Finite Element Analysis (FEM) approaches, which is impractical for our current project objectives.

We choose to design our simulation environment around the PyPullet physics engine, which is commonly used in robotics and reinforcement learning for rigid-multi-body simulations. This system architecture allows us to capture the dominant dynamics of our scene, allows for fast development cycles and lastly it poses an interesting research question, on whether such a degree of system approximation and abstraction suffices for robust sim2real transfer, given the application of explicit sim2real techniques.

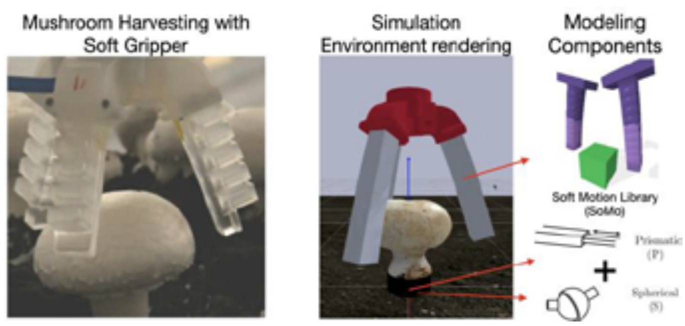

Figure 1 Real soft gripper prototype in the mushroom crop and the equivalent simulation environment.

We capture our scene's dominant dynamics through continuum mechanics formulations and multiple link-joint sequences for the soft robotic gripper, inspired by the Soft Motion Toolkit (SoMo)[1] For the mushroom-root deformation and material failure mode we combine a spherical with a prismatic joint controlled by a simple PD controller for emulating the linear elastic regions(see Figure 1). The proportional gains for all 4 DOFs of the mushroom-root system are computed based on the properties of a liner isotropic material. The failure mode occurs based on the Von-Mises stress criterion.

For fine-tuning the simulation and control parameters we conduct force-position experiments on real-world mushrooms, for determining the material elastic modulus terms and we also conduct step-response experiments on the finger of the real soft-gripper for system identification.

Figure 2 The simulation environment with the Panda Gripper and a randomized scene rendering.

The scene objects textures and colours as well as the scene lighting can arbitrarily change (see Figure 2) for avoiding over-fitting during training, thus increasing generalizing properties and ultimately making a sim2real transfer more likely.

III. FINDINGS/RESULTS

Based on real-world measurements of mushroom stiffness characteristics (see Figure 3) and the soft-gripper step responses we can conclude that our simulation framework is able to capture some dominant & critical dynamics of the mushroom-root system.

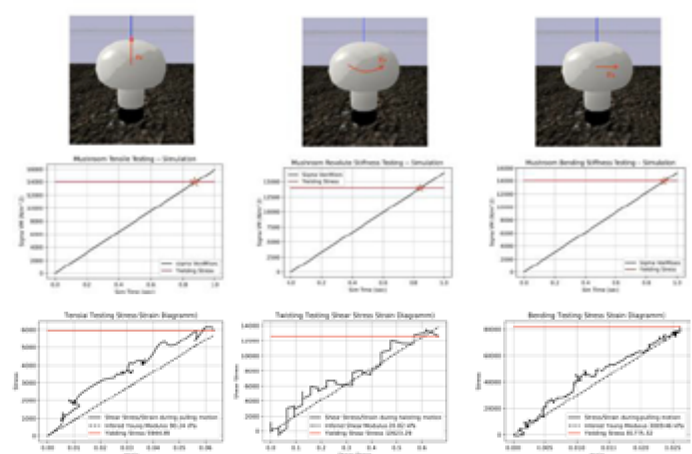

Figure 3 Mushroom root stiffness identification and replication in the simulation environment for the tensile, rotational and bending loads on the mushroom cap.

A very early naive sim2real transfer, without the use of any explicit technique, has been attempted without success, always leading to instabilities and abrupt motions of the real-world robot.

IV. DISCUSSION/CONCLUSIONS

We design a simulation framework for training and testing as a way to circumvent an analytical rule-based planning & control design approach, which would be probably unable to optimally handle each and every corner case for such a complex task (also known as the long-tail distribution problem). Designing a high-fidelity simulation environment for a real-world task, can also potentially be an equally or more complex & prohibitively expensive problem. A viable way to proceed is with a careful selection of the system's critical dominant dynamics and approximation hypotheses together with a set of explicit sim2real techniques.

It is important to note that the design of even a system with simplified-approximate dynamics is not trivial and requires a significant investment on development and some form of system identification processes as well. This is a significant bottleneck for the development and deployment of AI agents for real-world problems.

Another key observation is that the current workflow utilizes the simulation framework only during the training phase. As the simulation framework can be a representation and an abstraction layer of the real-work environment, which is also intuitive for humans, it could be utilized and be an integral part of the perception pipeline.

V. FUTURE PLAN/DIRECTION

Our work now focuses on refining and evaluation the domain randomization as a sim2real technique for this particular problem. For mitigating the problem of the discrepancy between the simulation rendering and the real-world video stream, we are evaluating domain adaptation techniques such as, feature mapping on the CNN embeddings and translation modules for homogenization of the CNN embeddings, regardless of a synthetic or real vision feed.

Based on the key insights we focus our research efforts on automating the generation of an ad-hoc simulation environment on physics-enhanced 3D scene reconstruction methods. The existence of such a simulation layer would allow for plan execution and trajectories generation in agent's "imagination" which can also be examined and evaluated by a human supervisor. These generated trajectories, waypoints and task-specific embeddings can be then translated to real-world robot action.

An intriguing possibility, which we are also examining, is the utilization of LLMs and Generative AI for performing this image-video-to-simulation-environment mapping.

REFERENCES

[1] M. A. Graule, T. P. McCarthy, C. B. Teeple, J. Werfel, and R. J. Wood, 'SoMoGym: A Toolkit for Developing and Evaluating Controllers and Reinforcement Learning Algorithms for Soft Robots', *IEEE Robot. Autom. Lett.*, vol. 7, no. 2, pp. 4071–4078, Apr. 2022, doi: 10.1109/LRA.2022.3149580.

Antonios Dimopoulos

Antonios received his BSc in October 2016 in Product and System Design Engineering from the University of the Aegean, and his MSc in April 2021 in Design & Engineering from Politecnico di Milano honoured with a 2-year merit-based scholarship. He started his career as an industrial design engineer in September 2015 when joined Innora/IKH, a company based in Greece, specialising in robotics and control systems. One year before his MSc graduation he joined TWI Hellas where he participated in more than 4 European projects, delivering solutions on Additive Manufacturing modelling and process optimisation. Continue working at TWI Hellas, in October 2021 Antonis started his PhD studies at Brunel University London and NSIRC under the guidance and supervision of Prof. Tat Hean Gan and Dr. Panagiotis Chatzakos. His research is sponsored by Lloyd's Register Foundation and focuses on the development of an innovative decision support platform for metal support structures optimisation of laser powder bed fusion systems.

Multi-response optimization and web-based visualization of Ti6Al4V support structures for laser powder bed fusion systems

Panagiotis Chatzakos[1], Tat-Hean Gan[1,2]
[1]TWI, [2]Brunel University London
2nd Year of PhD

Keywords: additive manufacturing; metal support structures; laser powder bed fusion; multi-response optimization;

I. INTRODUCTION

Laser Powder Bed Fusion (LPBF) is one of the most commonly used and rapidly developing metal Additive Manufacturing (AM) technologies for producing optimized geometries, complex features, and lightweight components, in contrast to traditional manufacturing, which limits those characteristics. However, this technology faces difficulties with regard to the construction of overhang structures and warping deformation caused by thermal stresses. For that reason, support structures are always required, since they anchor the part to the build plate, offer a suitable platform for the next layer to be built upon, and act as a heat sink that allows the part to cool at a more controlled rate. Therefore, producing an object without support structures results in distorted and collapsed parts, while the addition of unnecessary supports increases the post-processing, the time and effort needed to remove the supports, the risk to damage the part, and the amount of material required.

II. METHODOLOGY

The purpose of this study is to evaluate the various support and process parameters for metal LPBF and propose optimized support structures to minimize Support Volume, Support Removal Effort, and Warping Deformation. The optimization approach was based on the Design of Experiments (DOE) methodology and multi-response optimization, by 3D printing and studying overhang geometries from 0° to 45°. During the first round of experiments block type supports were investigated as shown in the following figure.

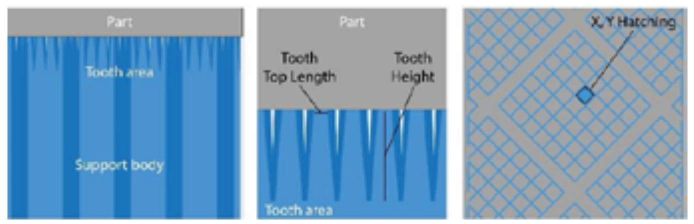

Towards the DOE, Response Surface Methodology (RSM) based on Central Composite Design (CCD) was used to perform the experiments and define the alternatives. 5 input parameters were used: Tooth Height, Tooth Top Length, X, Y Hatching, Laser Speed, and Overhang Angle, composed of 3 levels each, as shown in the following Table.

Parameter	Level 1	Level 2	Level 3
Tooth Height	1 mm	2.5 mm	4 mm
Tooth Top Length	0.05 mm	0.175 mm	0.3 mm
X, Y Hatching	0.5 mm	1.5 mm	2.5 mm
Laser Speed	1000 mm/s	1400 mm/s	1800 mm/s
Overhang Angle	0°	22.5°	45°

As a result, 43 unique configurations based on 3 specimens (0°, 22.5°, and 45°) were proposed for 3D printing. Specimens' geometry is shown next.

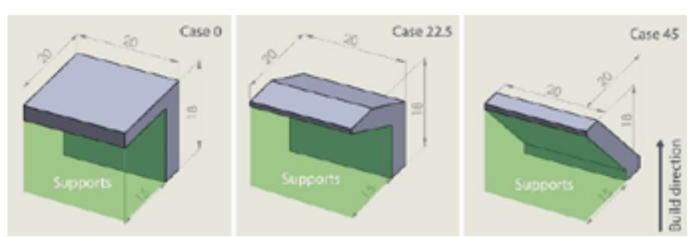

After the printings, three responses/outputs were evaluated: I) Support Volume by using existing online platforms, ii) Support Removal Effort by measuring the effort needed to remove the supports, and iii) Warping Deformation by measuring the displacement of the overhang surfaces using digital measuring tools. The collected data and the equations that occurred during the DOE, were used to develop a web-based Decision Support Platform for support structures optimization, able to detect the critical areas where supports are needed and propose optimized supports for easy removal, maintaining support volume and warping deformation to a minimum.

III. RESULTS AND DISCUSSION

The ANOVA results showed that most of the input parameters have a significant effect on Support Volume, Support Removal, and Warping deformation. It was found that as Tooth Height increases and Tooth Top Length decreases, Support Volume barely decreases. On the other hand, as X, Y Hatching increases, Support Volume decreases extremely, as shown in the next plots.

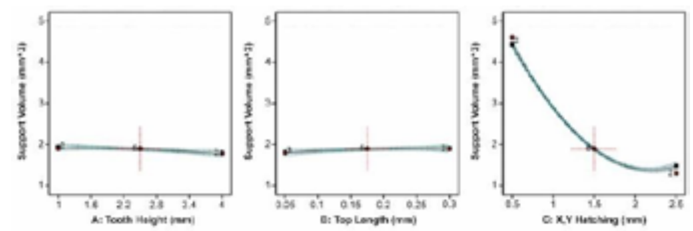

It can be also observed in the following plots that Support Removal Effort decreases for average values of Tooth Height, while as Tooth Top Length decreases, the removal effort decreases greatly. X, Y Hatching and Laser Speed barely affected the removal effort. It was also found that Support Removal Effort decreases as Overhang Angle increases.

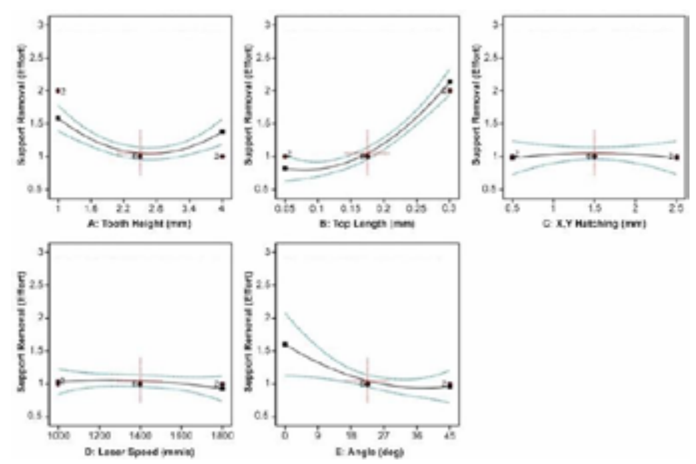

Regarding the Warping Deformation it was observed that warping significantly decreases as Overhang Angle increases, while the rest of the parameters barely affect the Warping Deformation, as shown in the next plots.

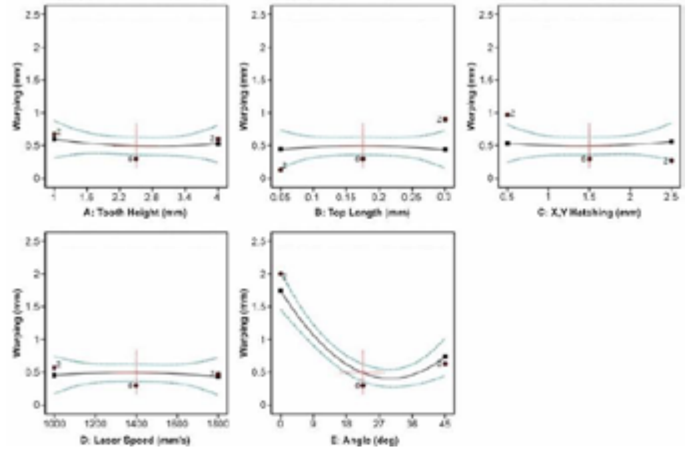

Overall, for 0° overhangs, the optimum solution was characterized by an average Tooth Height, large Tooth Top Length, low X, Y Hatching, and high Laser Speed, while for 22.5° and 45° overhangs, it was characterized by large Tooth Height, low Tooth Top Length, high X, Y Hatching, and high Laser Speed.

To that end, by using the exported data, DOE equations, and relevant optimization algorithms, a graphical and interactive environment of the web-based Decision Support Platform was developed as presented in the following figure.

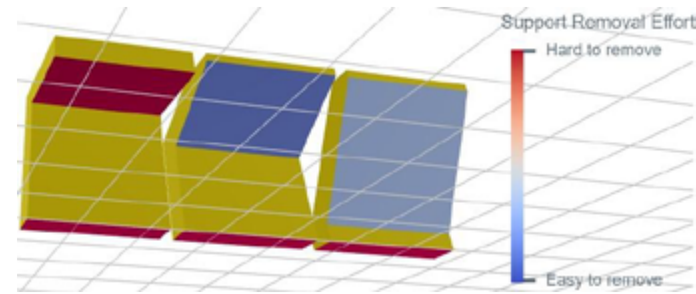

IV. FUTURE PLAN

Future work will include further research and experimentation on the various support and process parameters following a similar approach, to collect more data that would be useful towards the development of the proposed Decision Support Platform for metal support structures optimization.

ACKNOWLEDGMENTS

This publication was made possible by the sponsorship and support of Lloyd's Register Foundation (LRF). The work was enabled through, and undertaken at, the National Structural Integrity Research Centre (NSIRC), a postgraduate engineering facility for industry-led research into structural integrity, established and managed by TWI Ltd. through a network of both national and international universities.

REFERENCES

[1] Dimopoulos, A.; Zournatzis, I.; Gan, T.-H.; Chatzakos, P. Multi-Response Optimization of Ti6Al4V Support Structures for Laser Powder Bed Fusion Systems. J. Manuf. Mater. Process. 2023, 7, 22. https://doi.org/10.3390/jmmp7010022

Ali Alperen Bakir

Ali is a third year PhD student at Coventry University and NSIRC. He completed his BSc in mechanical engineering at Middle East Technical University. He then gained his MSc from Nottingham University, where he worked on the creep behaviour of additively manufactured Inconel 718. This publication was made possible by the sponsorship and support of Lloyd's Register Foundation. The work was enabled through, and undertaken at, the National Structural Integrity Research Centre (NSIRC), a postgraduate engineering facility for industry-led research into structural integrity established and managed by TWI through a network of both national and international Universities. Lloyd's Register Foundation helps to protect life and property by supporting engineering-related education, public engagement and the application of research.

Structural integrity assessment of cold spray repaired high-strength aluminium alloy 7075 specimens

Xiang Zhang[2], Matthew Dore [1,2], Phil McNutt[1], Kashif Khan[2]
[1]TWI, [2]Coventry University
3rd Year of PhD

Keywords: Cold spray, repair, aluminium alloy 7075, structural integrity

I. INTRODUCTION

Aluminium Alloy (AA) 7075 is widely used in the aerospace industry owing to its high strength-to-weight ratio and durability. Nonetheless, these components are prone to damages during their operational lifespan, such as corrosion pits, and fatigue cracks. Repairing such components becomes crucial to minimise costs, maintenance time, and environmental impact. However, due to the temperature and oxidation sensitivity of this material, and the tendency to form micro-cracks during fusion welding, high temperature processes are not considered viable [1].

Cold spray (CS) is a solid-state deposition method, in which microscopic metal particles are accelerated to supersonic velocity using an inert gas such as nitrogen or helium. At a critical velocity, these particles have sufficient kinetic energy that upon impact with a suitable substrate they plastically deform and become metallurgically bonded to the substrate. As this is a solid state process, the temperature is kept below the melting point of the deposited alloy. This helps to eliminate the negative consequences that may arise from utilising high-temperature processes. This process is predominantly used for deposition of functional coatings, which may improve properties such as wear and corrosion resistance, but following the developments over the last two decades, it is also used for additive manufacturing and repair applications.

The mechanical performance of CS repaired specimens is a concern due to the porosity, interface defects and lack of ductility. Also, the effects of pre and post deposition heat treatments are yet to be fully understood. Therefore, this project aims to explore the structural integrity of CS repaired AA7075 specimens by studying the repair geometry and the effect of post-deposition heat treatment.

II. METHODOLOGY

Gas-atomised AA7075 powders were deposited onto an AA7075-T651 substrate using nitrogen as the process gas. Parameter development trials were performed, varying gas pressure and temperature, and the combination of 500°C and 6MPa was chosen. This selection was based on the area fraction of porosity, deposition efficiency, and qualitative interface analysis using image processing of optical micrographs.

To assess the structural integrity of the repaired specimens, microstructure analysis, adhesion test (ASTM C633) and tensile test (ASTM E8) were conducted. Two types of repaired specimens, namely through width repair and centre dent repair, were tested (Figure 1). The through width repaired samples were heat treated in an air furnace after the deposition, as detailed in Table 1. During the tensile test, the displacement was recorded using extensometer.

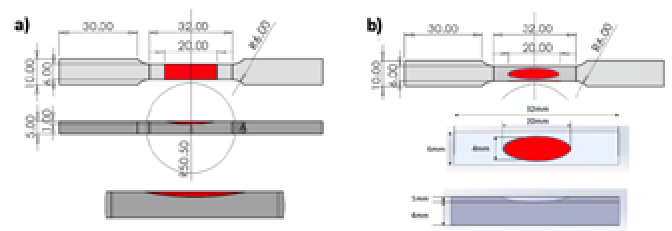

Figure 1 Schematic of the tensile specimens with a) groove repair, b)centre dent repair.

Table 1 Post-deposition heat treatment conditions

Specimen	Heat-Treatment Condition
SHT+T6	450°C (12h) + 121°C (24h)
Annealed	400°C (3h)

III. RESULTS

The process parameter selection resulted in a coating without any interfacial defects and with the area density of porosity was less than 1% (Figure 2).

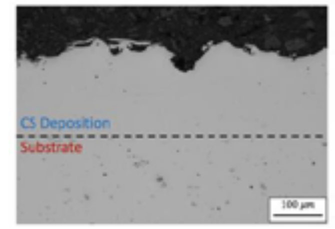

Figure 2 Microstructure of a cold spray deposition with the selected process parameters.

Figure 3 shows the back-scattered electron images of CS samples. SEM analysis of the as-deposited specimen revealed that the inhomogeneous microstructure of the gas-atomised powder was maintained after the deposition. Following the Solution Heat Treatment (SHT) and annealing, the segregated elements were mostly dissolved into the solid solution, leading to a more homogenised matrix. However, the microstructure still displays bright, needle-shaped precipitates. Additionally, defects were observed, resulting from incomplete particle compaction.

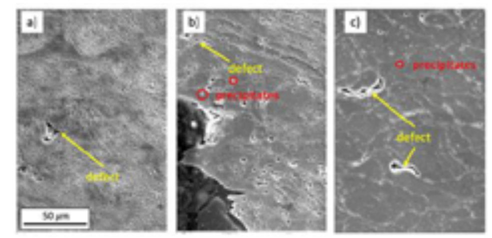

Figure 3 SEM images of cold spray depositions in a) as-deposited, b)annealed c)SHT+T6 conditions.

The tensile properties of the specimens, subjected to different heat treatment conditions, were compared based on their load-displacement curves, as shown in Figure 3. The load drops in the repaired samples indicate the corresponding points of repair failure. The SHT condition resulted in an improvement in the strength of the cold spray repair. However, annealing the repaired samples led to a significant decrease in strength, despite an increase in ductility.

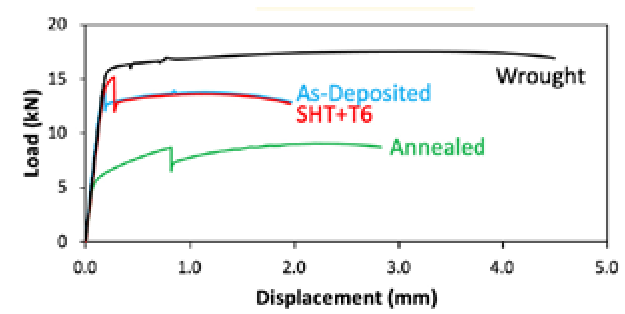

Figure 4 Load-displacement curves of specimens with different post deposition heat treatment conditions.

To further investigate the potential of CS repair performance, and making the repair geometry more representative of how a repair would typically be applied, the repair geometry was modified from a groove repair to a centre dent repair.

Consequently, the load drop after the repair failure was eliminated, as demonstrated in Figure 4. The centre dent samples carried roughly 10% higher load, indicating improved strength.

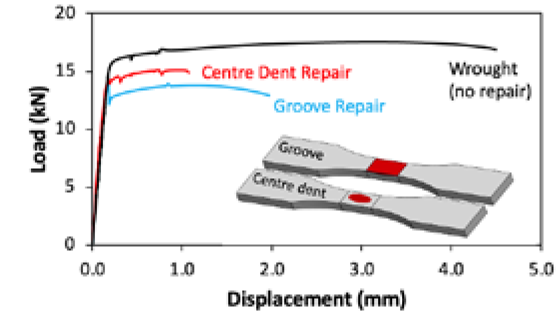

Figure 5 Test measured load-displacement curves of specimens with different repair geometries.

IV. DISCUSSION AND CONCLUSIONS

To minimise defects such as porosity and lack of bonding at the coating/substrate interface, parameter development trials were successfully performed, resulting in a significant reduction in porosity and marked improvement in the quality of the coating/substrate interface, resulting in a relatively high adhesive strength.

As-deposited samples had low ductility due to the defects between the powder particles. An increase in strength is observed after the SHT which is mostly due to the improved interparticular bonding and precipitation hardening during the ageing. However, since the pores could not be eliminated during SHT, the repair still had brittle behaviour. Annealed specimens on the other hand had reduced strength because of coarse precipitates present in the material matrix.

The strength of the repaired samples was improved by changing the repair geometry as a result of eliminating the free edge effect.

V. FUTURE PLAN

Further investigation is needed to understand the fracture mechanism of repaired specimens under tensile loading. Also, fatigue testing will be conducted to assess the mechanical performance of the repaired specimens under cyclic loading since this material widely used for aircraft wings which experience cyclic loading in its service life. Additionally, further porosity analysis will be performed to understand the fracture mechanism.

REFERENCES

[1] D. Peng, R. Jones, N. Matthews, and C. CaTang, 'On the role of the interface on the damage tolerance and durability of cold spray repairs to AA7075-T7351 aluminium alloy wing skins', Appl. Surf. Sci. Adv., vol. 3, p. 100044, Mar. 2021, doi: 10.1016/j.apsadv.2020.100044.

Ahamed Ameen
Doctoral student with NSIRC, TWI and Coventry University, Ahamed is working on the microstructural optimisation of wire-fed Direct Energy Deposition (DED) of low alloy steels. This work is sponsored by Lloyd's Register Foundation. Lloyd's Register Foundation helps to protect life and property by supporting engineering-related education, public engagement and the application of research.

Wire-fed DED of low carbon steels – Influence of process control methods on properties and microstructure

Ahamed Ameen[1,2], Joanna Nicholas[1], Vit Janik[2], Cui Er Seow[1], Xiang Zhang[2]
[1] TWI, [2] Coventry University
3rd Year of PhD

Keywords: wire arc additive manufacturing, low alloyed steels

I. INTRODUCTION

Additive manufacturing (AM), in contrast to traditional manufacturing, fabricates 3-dimensional products in a layer-by-layer fashion of material addition. Metal additive manufacturing (MAM) has branched into different processes such as Direct Energy Deposition (DED), powder bed fusion, binder jetting, laminated object manufacturing, among others, with the help of different feedstock types such as powders, wire, and sheets. The choice of technology depends on the material, complexity, and size of the object being produced. Wire-fed DED is one such MAM process, in which the wire feedstock is melted by an arc or laser energy source, to be deposited over a substrate, resulting in the creation of near-net shape parts. Wire-fed DED is characterised by high deposition volume, material usage efficiency, and deposition rates while the process suffers from limitations such as low geometrical accuracy, and inhomogeneity in material properties and microstructure.

In this work, two low-carbon steel walls (C-Mn) were deposited with the same feedstock (ER70S-6) and heat input parameters but with two different process control methods. For the first thick wall deposition, a maximum interlayer surface temperature of 250°C was adopted before depositing the next layer. For the second deposition, a constant dwell time of 200 seconds was allowed before subsequent material deposition. In-process temperature measurements were made across different regions of the wall to obtain the cooling rate at that particular region to be correlated with microstructure and material properties, analysed by testing the samples extracted from the walls.

II. EXPERIMENTAL DESIGN

Two thick/wide walls of dimensions 26mm x 325mm x 200mm were deposited on low carbon steel plates with solid wire ER70S-6 feedstock by wire-arc DED method. The deposition was carried out in an alternating fashion by adopting an oscillation strategy and the process parameters adopted for deposition are given in table 1. Temperature measurements were made using K-type thermocouples (0.8 mm diameter calibrated at TWI), inserted into the molten pool, and recorded with the pico-logger.

Table 1: Process parameters for Wire-Arc DED depositions

Process Parameter	Current (I)	Voltage (V)	Traverse speed (mm/s)	Wire speed feed (m/min)	Contact Tip to Work Distance (mm)	Gas flow rate (l/min)	Heat input (kJ)
Value	204	20.6	1.95	8.4	15	16	2.406

In the as-deposited condition, the walls were extracted from the substrate and subjected to non-destructive testing by X-ray radiography method to identify macro-defects presence.

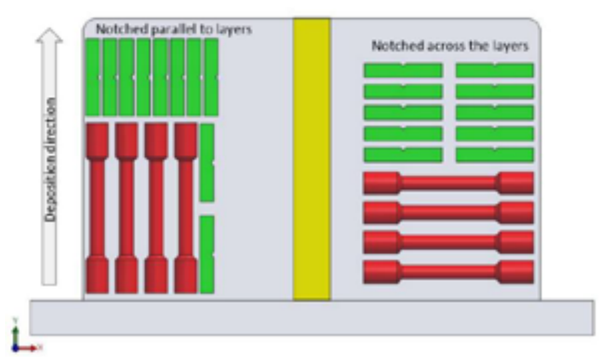

Figure 1: Extraction of mechanical testing and microstructural specimens from the as-deposited low carbon steel walls

Specimens for mechanical testing and microstructural examination were extracted from different orientations as shown in Figure 1. Tensile and Charpy impact samples were extracted from the horizontal and vertical orientations of the wall while specimens for microstructural analysis were extracted across the wall height.

III. RESULTS

1. Thermo-couple measurements

By wire-arc DED method, the oscillating strategy was adopted for depositing 26mm thick layers over the substrate. After a wall height of 40mm was achieved, a thermo-couple was placed over it and subsequent deposition was carried out to embed the thermo-couple in the wall and record the thermal history during processing. Placement of thermo-couples in such manner was repeated after wall heights of 100mm and 160mm were reached, thus recording thermal history from three different regions of the wall. Thermal history recorded from top region for walls 1 and 2 are shown in Figure 2.

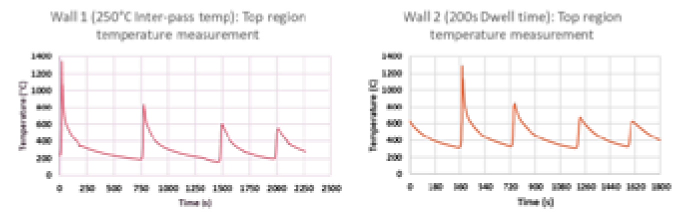

Figure 2: Temperature measured by Thermo-couple placement from the top region

2. Tensile testing

Blanks extracted from the walls were prepared for tensile testing according to BS-EN ISO 6892 standards. The tensile specimens were extracted parallel (vertical) and across (horizontal) to the deposition direction to check the presence of anisotropy in mechanical properties.

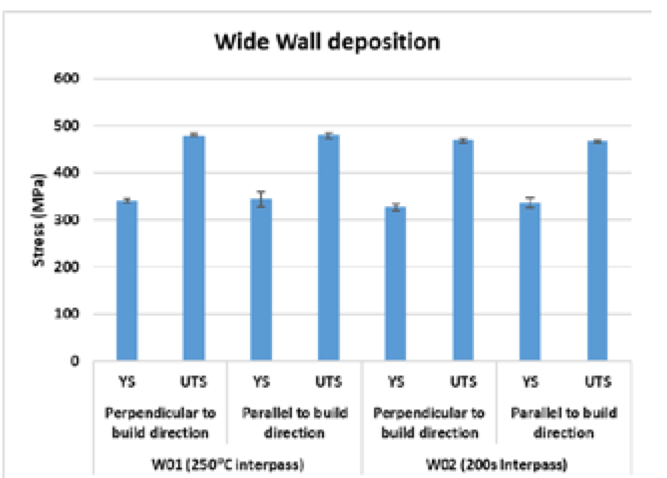

Figure 3: CCT diagram calculated for base composition with Thermo-calc

Upon testing the samples, it was observed that the tensile strength of the material is consistent across the sampling direction while comparing with different process controls, a small difference (~10MPa) in tensile strength was observed between samples extracted from two walls. The yield and tensile strength values for both walls across different orientation is shown in Figure 3.

3. Microstructural examination

Electron Back Scattered Diffraction (EBSD) analysis was performed on samples extracted across the deposition direction, from regions adjacent to the thermo-couple insertion, for analysing grain statistics. The presence of inter-layer regions in the microstructure with bands of coarse and fine equiaxed ferrite grains of average size 12µm and 9µm respectively, were observed, irrespective of the processing condition of the walls, as shown in Figure 4.

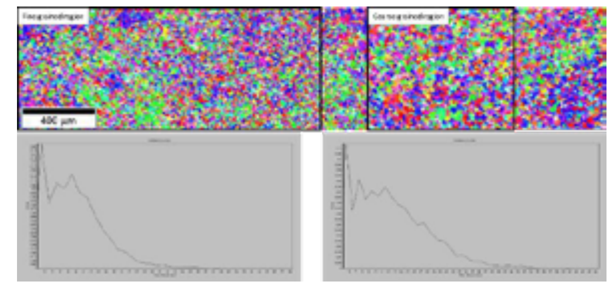

Figure 4: Inverse pole figure maps taken through the interlayer region of width 2mm

IV. DISCUSSION/CONCLUSIONS

The walls processed by two different process methods exhibit comparable mechanical properties and consistent hardness across the build profile. While microstructural evaluation using EBSD shows inter-layer region presence for both the walls denoting negligible change with the microstructure. This suggests inter-layer dwell time method can be adopted for better productivity during deposition.

V. FUTURE PLAN/DIRECTION

Adopting the inter-layer dwell time control for wire-arc DED processing, further deposition trials are to be carried out by varying the feedstock composition. This will be compared to previous depositions to evaluate the change in material properties.

VI. REFERENCES

[1] Hashmi, M. (2014). Comprehensive materials processing : 13 volume set.

[2] Greer, C., Nycz, A., Noakes, M., Richardson, B., Post, B., Kurfess, T., & Love, L. (2019). Introduction to the design rules for Metal Big Area Additive Manufacturing. Additive Manufacturing, 27(C)

VII. ACKNOWLEDGEMENTS

This publication was made possible by the sponsorship and support of Lloyd's Register Foundation (LRF) and Coventry University. The work was enabled through, and undertaken at, the National Structural Integrity Research Centre (NSIRC), a postgraduate engineering facility for industry-led research into structural integrity established and managed by TWI through a network of both national and international Universities

Yixiang Jin

Yixiang is a PhD candidate at Lancaster University with a background in materials and chemistry. He holds an MSc(Eng) degree in Aerospace Materials from the University of Sheffield. Yixiang's research focuses on the environmental cracking of additively manufactured materials.

Examination of environmental cracking in additively manufactured materials

Briony Holmes[1], Pedro Rivera-Diaz-del-Castillo[2]
[1]TWI, [2]University of Lancaster
2nd Year of PhD

Keywords: Additive manufacturing, Laser powder bed fusion, Hydrogen embrittlement, 316L stainless steel

I. INTRODUCTION

Additive Manufacturing (AM) technologies are rapidly maturing and while basic properties such as strength and Charpy impact toughness are widely reported, the environmental cracking behaviour is largely unknown. Environmental cracking mechanisms like stress corrosion cracking and hydrogen embrittlement are insidious failure mechanisms which occur where a susceptible microstructure is combined with a corrosive environment and stress, potentially leading to catastrophic failure and loss of life. Research is urgently needed to establish if AM materials behave similarly to traditional materials in terms of environmental cracking mechanism(s) and therefore identify if standard approaches to prevent these failures are appropriate for AM components.

Hydrogen as clean renewable energy can be a new way to store and transfer electricity. It may also have the potential to replace fossil fuels. Hence, the storage of hydrogen has been an area with growing interest in research. However, hydrogen atoms may enter the alloy and lead to the degradation of mechanical properties, this phenomenon is known as hydrogen embrittlement [1]. 316L stainless steel (SS) can be employed as high pressure or liquid hydrogen containers due to its good low temperature performance and high corrosion resistance. However, the influence of additive manufacturing on the hydrogen embrittlement of 316L SS are still unclear. The mechanical properties of AM 316L SS are largely affected by the dislocation network formed during the large and repetitive temperature variation of the process, the network might also change the mechanisms of hydrogen-assisted cracking. It is also reported that sub-grain boundaries formed by dislocation networks in the materials might act as the fast transportation channel of hydrogen atoms[2]. They may also be responsible for the strain-induced martensite transformation [3] and hence may affect the performance under hydrogen conditions. This project is now focusing on the differences in the hydrogen embrittlement that may occur due to those unique microstructures of AM 316L SS manufactured by laser powder bed fusion (L-PBF) process.

II. DESIGN/METHODOLOGY/APPROACH

Modelling, Mechanical testing and Characterisation approaches will be employed to investigate the hydrogen behaviour in L-PBF 316L SS.

A collection of published data on hydrogen embrittlement on L-PBF steels has been created for machine learning.

The sample will be charged with hydrogen in a NaCl solution to simulate seawater environment. The hydrogen charging and egressing process will be modelled by Finite Difference Modelling (FDM) and Finite Element Modelling (FEM) methods, and the results will be verified by thermal desorption spectroscopy experiments.

Mechanical tests will be carried out on charged samples to evaluate any mechanical degradation caused by hydrogen embrittlement of L-PBF 316L SS. The results will be combined with the modelled hydrogen profile to analyse any hydrogen damage.

Various characterisation methods, including optical microscopy, SEM and X-ray/neutron diffraction will be employed to investigate the microstructural changes caused by hydrogen.

III. FINDINGS/RESULTS

An FDM model for a 1D case of hydrogen diffusion with consideration of hydrogen traps in the alloy has been established. The hydrogen profile of samples under various charging conditions has been created. The accuracy of the results is yet to be verified. Notched mechanical test specimens of L-PBF 316L SS have been machined.

IV. DISCUSSION/CONCLUSIONS

The hydrogen diffusion model showed a quite slow diffusion coefficient of hydrogen in 316L SS. Although Lin et al. [2] reported that the diffusion coefficient of L-PBF 316L SS is much larger than that of wrought 316L SS, it is still nearly impossible to fully charge a sample with over 2 mm thickness at room temperature. The simulation suggested that the hydrogen charging for any 316L SS should be carried out at elevated temperatures. However, for thicker samples over 5 mm, hydrogen will still only be present at the near-surface area of the sample in the acceptable charging time (within 30 days). For any mechanical tests carried out on these samples, embrittled and normal areas should be observed on fracture surfaces. The modelled hydrogen profile will help to distinguish the boundary of these areas.

V. FUTURE PLAN/DIRECTION

Future work will focus on verifying the accuracy of the FDM model through comparison with experimental results obtained from thermal desorption spectroscopy. The notched mechanical test specimens will be used to evaluate the hydrogen embrittlement at an area of stress concentration, the results will be analysed to study the role of the sub-grain networks of L-PBF manufactured materials in hydrogen embrittlement.

The results will be combined with the modelled hydrogen profile to analyse the hydrogen damage and identify hydrogen behaviour in L-PBF manufactured 316L.

SEM and neutron/X-ray diffraction techniques will be employed to characterise the microstructural changes caused by hydrogen.

The collected data set will be used to train a machine learning model which aims to predict the stress-strain curve of hydrogen charged L-PBF manufactured steel based on the composition, heat treatment, L-PBF parameters and charging conditions. The prediction of the model will be compared with the experimental data to verify its accuracy.

The results from all approaches will be summarised and analysed to create and verify a physical model of hydrogen embrittlement mechanisms in L-PBF 316L. Machine learning will be employed to assist the study. By the end of the project, a mechanistic understanding of hydrogen embrittlement in L-PBF 316L SS is aimed to be established.

VI. ACKNOWLEDGEMENTS

This publication was made possible by the sponsorship and support of Lloyd's Register Foundation. The work was enabled through, and undertaken at, the National Structural Integrity Research Centre (NSIRC), a postgraduate engineering facility for industry-led research into structural integrity established and managed by TWI through a network of both national and international Universities. Lloyd's Register Foundation helps to protect life and property by supporting engineering-related education, public engagement and the application of research.

REFERENCES

[1] K. M. Bertsch, A. Nagao, B. Rankouhi, B. Kuehl, and D. J. Thoma, "Hydrogen embrittlement of additively manufactured austenitic stainless steel 316 L," *Corros Sci*, vol. 192, p. 109790, Nov. 2021, doi: 10.1016/j.corsci.2021.109790.

[2] J. Lin, F. Chen, F. Liu, D. Xu, J. Gao, and X. Tang, "Hydrogen permeation behaviour and hydrogen-induced defects in 316L stainless steels manufactured by additive manufacturing," *Mater Chem Phys*, vol. 250, p. 123038, Aug. 2020, doi: 10.1016/j.matchemphys.2020.123038.

[3] Y. Hong *et al.*, "Strain-induced twins and martensite: Effects on hydrogen embrittlement of selective laser melted (SLM) 316 L stainless steel," *Corros Sci*, vol. 208, p. 110669, Nov. 2022, doi: 10.1016/j.corsci.2022.110669.

Siddharth Patil

Post graduate researcher from NSIRC and Coventry University. Siddharth completed MSc in Welding Engineering from Cranfield University in the year 2018. Siddharth's research topic is 'Development of wire arc directed energy deposition (DED) process for consistent bead shape and intersection geometry analysis'. The main aim of his research is process optimisation and consistent bead geometry through control methods in low carbon steels. This publication was made possible by the sponsorship and support of Lloyd's Register Foundation. Lloyd's Register Foundation helps to protect life and property by supporting engineering-related education, public engagement and the application of research. The work was enabled through, and undertaken at, the National Structural Integrity Research Centre (NSIRC).

Effect of process parameters on bead geometry of low carbon alloy steel manufactured by wire arc directed energy deposition (DED)

Cui Er Seow[1], Xiang Zhang[2]
[1]TWI, [2]Coventry University
3rd Year of PhD

Keywords: Wire arc DED process, low carbon steel, process parameters, bead geometry

I. INTRODUCTION

Wire arc Directed Energy Deposition (Wire arc DED) is an advanced manufacturing technology that utilises arc welding processes to fabricate three-dimensional (3D) metal parts layer by layer from metal wire feedstock. Understanding the effect of process parameters on bead geometry is crucial for achieving a stable and repeatable Wire arc DED process. Variations in bead geometry can lead to inconsistencies in part quality and may require additional post-processing steps, such as machining or heat treatment, to achieve the desired specifications[1]. By investigating the effect of process parameters on bead geometry, Wire arc DED process can be optimize for different materials, part geometries, and desired properties. Suryakumar et al. [2] employed regression analysis to generate a bead geometry model, taking into account the width and height of the beads in relation to feed rate and travel speed. Higher electrical current levels generally result in a higher deposition rate of the material, which can affect bead geometry. Increasing current may lead to wider and taller beads, which can consequently impact the overall geometry of the 3D object being manufactured [3]. The interlayer temperature affects the viscosity and flow of the molten material, which in turn influences the bead geometry of Al-6.3%Cu alloy. A longer contact tip to work piece distance (CTWD) may lead to a wider and shallower bead due to the broader distribution of heat.

II. DESIGN/METHODOLOGY/APPROACH

Wire arc DED samples were manufactured using an OTC Daihen FD-B4 six-axis robot, fitted with a robot controller, Daihen OTC Welbee P500L Synchro-feed MIG/MAG arc welding power source, wire feeder and welding torch, as shown in Figure 1. Experiments utilized shielding gas (80% argon and 20% carbon dioxide mix) at a constant flow rate of 19 l/min, ER70S-6 feedstock wire with 1.2 mm diameter, and EN 10025 S275JR rolled plate as the substrate.

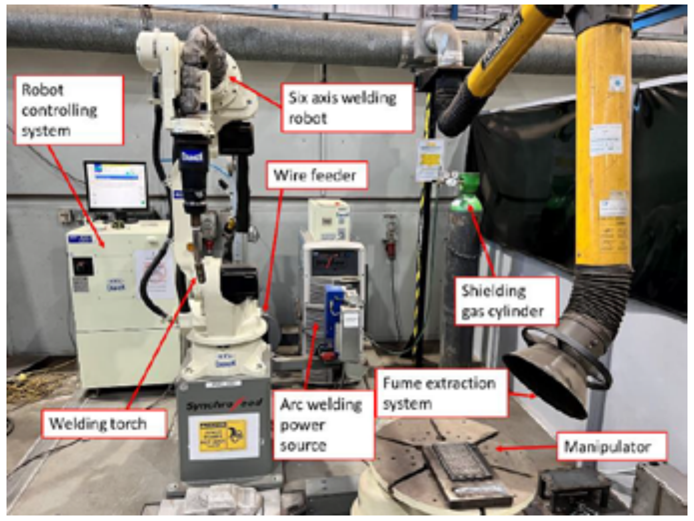

Figure 1 Wire arc DED process setup

The Box-Behnken design (BBD) is a three-level fractional factorial design that incorporates aspects of two-level factorial and incomplete block designs. It is a quadratic design with experimental points at the midpoints of a cube's edges and in the centre. The Box–Behnken designs make it possible to study sequentially the effect of the various factors of the design if, during the study of the first factors, the other factors are maintained at a constant level. The total number of experiments is determined as $N = 2z(z-1) + C_0$ where z is the number of experimental factors and C0 is the number of centre points of level (0, 0, 0, and 0) to complete the design. In current research z is 4 and C0 is 3. Parameters and their levels mentioned in Table 1.

Parameters	Levels		
	-1	0	1
Current, I (A)	170	190	210
Travel speed, v (mm/s)	9.2	10	10.8
CTWD, d (mm)	10	15	20
Interlayer temp., t (°C)	150	200	250

Table 1 Parameters and their levels

III. FINDINGS/RESULTS

This section will explore the qualitative and quantitative outcomes obtained from the single bead multi layered specimen evaluations. Minitab 18, a statistical software, was utilised to create mathematical models to obtain max. usable width (W) and height (H). Figure 2, represents section view of the one of the deposited sample and 3D scanned image of the same sample.

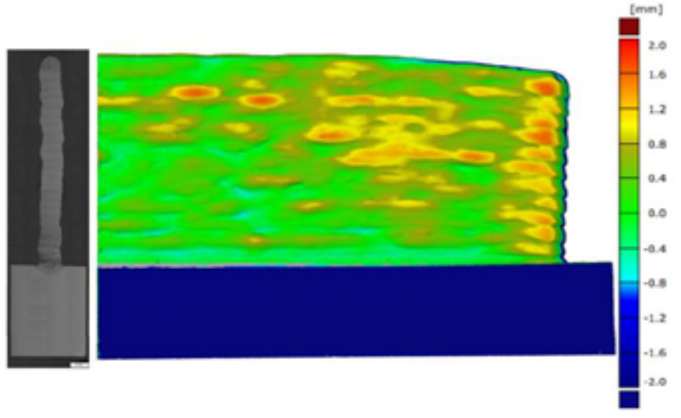

Figure 2 Section view (left) and 3D image (right) of the sample

From the main effect plot in Figure 3, of the four factors considered, CTWD was observed to have the largest impact on max. usable width, which decreases with increasing CTWD. The effects of current, interlayer temperature and travel speed are smaller in comparison to CTWD. From the main effect plot in Figure 4, current was observed to have the largest impact on max. usable height. Travel speed and CTWD have less impact when compared with current. Interlayer temperature was observed to have no significant effect on max. usable height.

IV. DISCUSSION/CONCLUSIONS

Elevated current levels contributed to an increase in heat generation, subsequently leading to the formation of a more extensive molten pool. This larger molten pool directly influenced the deposited bead, resulting in a greater bead height. Furthermore, an increased CTWD causes an augmentation in arc voltage, thereby elevating energy density. This primarily results in a more expansive and broader molten pool, significantly impacting bead width. To optimize bead dimensions, both width and height, it is imperative to consider the synergistic effects of current and CTWD. The optimal combination comprises a low CTWD (-1) and a medium current (0) level, which together facilitate the attainment of the most suitable bead geometry.

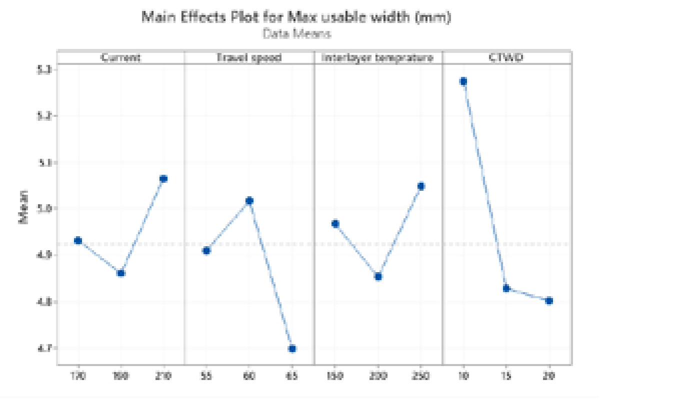

Figure 3 Main effect plot of max. usable width against 'I', 'v', 't' and 'd'

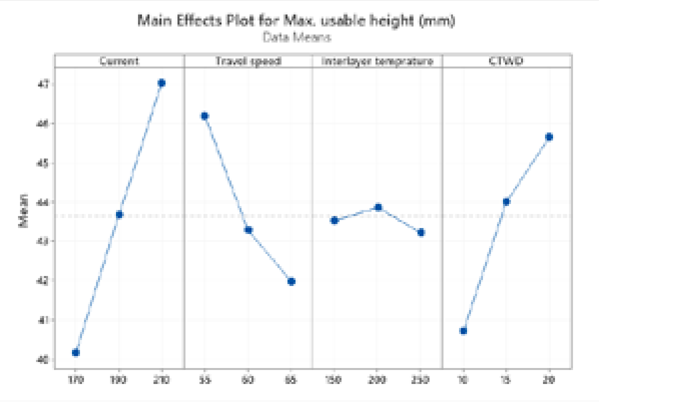

Figure 4 Main effect plot of max. usable height against 'I', 'v', 't' and 'd'

V. FUTURE PLAN/DIRECTION

Use of research data to study and achieve consistent bead geometry at intersections.

REFERENCES

[1] H. Stinson, R. Ward, J. Quinn, and C. McGarrigle, "Comparison of properties and bead geometry in mig and cmt single layer samples for waam applications," *Metals (Basel)*, vol. 11, no. 10, Oct. 2021, doi: 10.3390/met11101530.

[2] S. Suryakumar, K. P. Karunakaran, A. Bernard, U. Chandrasekhar, N. Raghavender, and D. Sharma, "Weld bead modeling and process optimization in Hybrid Layered Manufacturing," *CAD Computer Aided Design*, vol. 43, no. 4, pp. 331–344, Apr. 2011, doi: 10.1016/j.cad.2011.01.006.

[3] D. Ding, Z. Pan, D. Cuiuri, and H. Li, "Wire-feed additive manufacturing of metal components: technologies, developments and future interests," *International Journal of Advanced Manufacturing Technology*, vol. 81, no. 1–4. Springer London, pp. 465–481

Francesco Careri

Francesco is a PhD student at the University of Birmingham and TWI Ltd through the EPSRC CDT in Topological Design and the National Structural Integrity Research Centre (NSIRC). His project, funded by the European Union's Horizon 2020 research and innovation programme, is focused on the development of Additive Layer Manufacturing technology as a potential means to produce thin features and more efficient Al-alloys heat exchangers for aerospace applications. Francesco obtained his MSc degree in Mechanical Engineering at the University of Calabria in Italy. During his final year project, he collaborated as a visiting student at the AMPlab, University of Birmingham, where he carried out experimental and numerical analyses of different post-processing strategies for Ni-superalloys structures fabricated using Direct Energy Deposition.

Development of post thermal treatments for L-PBF A20X

Raja H. U. Khan[1], Moataz M. Attallah[2]
[1]TWI, [2]University of Birmingham
3rd Year of PhD

Keywords: Additive Manufacturing; High-strength Al Alloy; Post Thermal Treatments.

I. INTRODUCTION

Additive Manufacturing (AM) of high-strength alloys with topological optimisation can produce lightweight, high-performance parts and make a difference in industrial sectors such as space, aerospace and automotive [1]. The additively manufactured (AMed) high-strength AlCu-based alloy reinforced with TiB2 commercially known as A20X™, is a good alternative to cast Al alloys because of its superior mechanical properties at high temperatures and corrosion performance [1-2]. The as-AMed A20X™ has superior properties, especially at elevated temperatures compared to AlSi10Mg which is currently used in most aluminium (Al) AM parts manufacturing used in various industrial sectors. Unfortunately, standard heat treatments (HTs), perfectly developed for cast or wrought materials, are not compatible with AMed Al alloys due to the difference in as-fabricated materials' microstructure. The as-built Al alloys have fine-grained microstructure with no apparent segregation, unlike the materials produced through conventional cast or wrought manufacturing techniques. Attempts to the analysis of the influence of standard HTs and the development of modified HTs were made but the available data is still not consistent. The aim of this study is to develop a novel HT for A20X™ material in order to enhance the mechanical properties and overcome the materials' performance issue. The mechanical performance in terms of strength and fatigue of the newly developed HT was compared with the standard HT for cast alloys and the HTs available in the market for AMed A20X™ material.

II. DESIGN/METHODOLOGY/APPROACH

A customised version of A20X™ (AlCu-TiB2) alloy with less amount of Ti and B, commonly known as A207, was used during this study. A Concept Laser M2 Cusing laser powder bed fusion (L-PBF) machine with 400W laser was used during the fabrication of A20X™ samples.

The optimisation and analysis of the HT parameters were carried out in several stages. The development of the new HT i.e. Solution and Artificial Ageing was carried out using fixed temperatures. In particular, a fixed Temperature of 520°C for up to 24 hours was used for the Solution treatment. The best Solution HT conditions were then subjected to artificial ageing at 170°C up to 24h. The best combination in terms of solution and ageing conditions was identified via hardness analysis. Cuboid, tensile and fatigue test samples were fabricated using L-PBF optimised process parameters then treated using; i) newly developed post thermal treatment, ii) standard HT and iii) commercially available HT. The microstructure evolution (grains and phases) during the post thermal treatments was assessed via optical and SEM microscopes. Finally, the mechanical properties i.e. tensile and fatigue were tested at room temperature.

III. FINDINGS/RESULTS

The manufacturing map to ensure a defect-free AlCu-TiB2 material with a density comparable to the bulk material obtained by traditional manufacturing methods was found and the optimal process parameters for L-PBF were defined through further microhardness, surface roughness and SEM density analyses. The optimal parameters were used to generate the bulk samples for the development of HT. Fig. 1 is showing the typical microstructure of as-built A20X™ material highlighting the presence of Cu segregation to the grain boundaries and the formation of TiB2 randomly dispersed in the matrix. Furthermore, some TiB2 clusters were found.

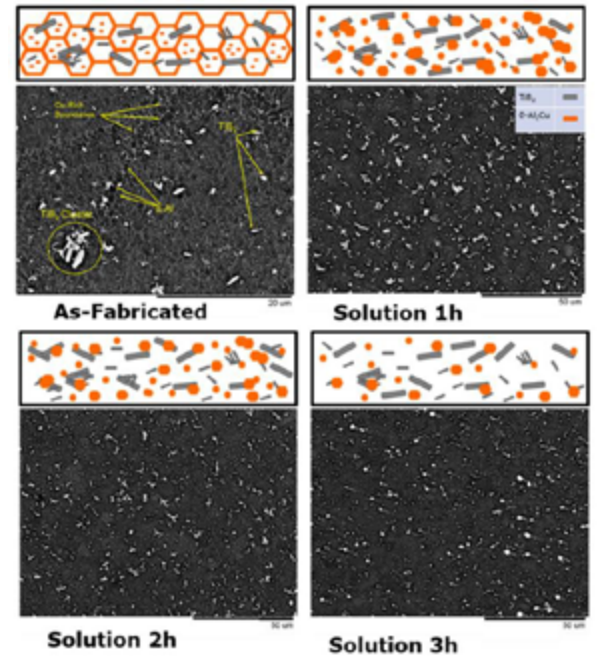

Figure 1. Microstructure and intermetallic particle analysis of as-fabricated and Solution HTed A20X™.

The Solution treatment was intended to dissolve Cu segregation into the Al matrix (Fig. 1). The Cu dissolution is important to enhance the formation of ϑ' and Ω phases during artificial ageing.

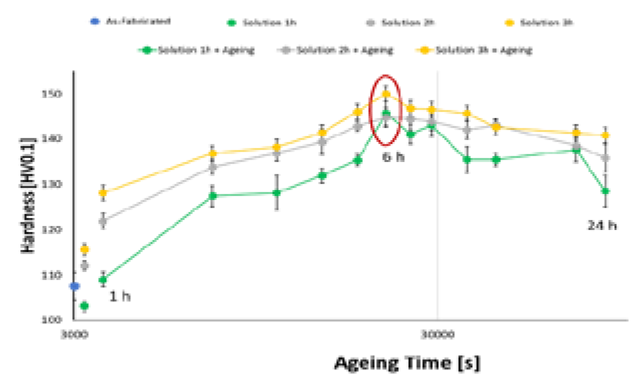

Figure 2. Hardness data for A20X™ with different HTs.

In particular, the most decrease in phases' precipitation and segregation was found during the first hours of Solution treatment. Hardness analysis was used to set the best candidates in Solution treatment and the final developed HT after ageing treatment. The results presented in Fig. 2 highlighted 3h as the best Solution time and a peak ageing time of 6h for artificial ageing. Therefore, new HT conditions were chosen accordingly. The mechanical performance of A20X™ material with new HT compared to standard HT is represented in Fig. 3. All HTs maximise the yield and ultimate tensile strength of the material with a decrease in elongation. The newly developed HT is characterised by higher elongation (Fig. 3a). Finally, a comparison of fatigue performance at room temperature and fixed load of 180MPa (Fig. 3b) and the analysis of surface fracture were performed.

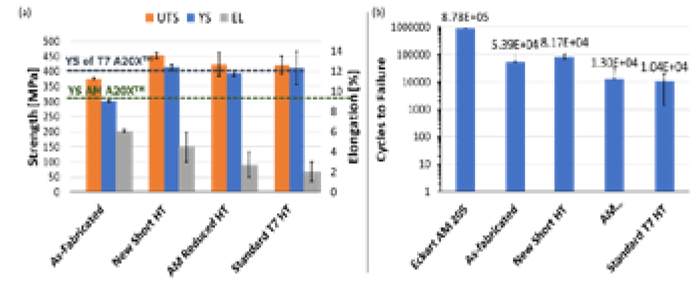

Figure 3. (a) Tensile and (b) Fatigue data of A20X™ with different HTs [1, 4].

The results highlighted the presence of high Thermal Induced Porosity (TIP) for the standard T7 HT and the commercially available HT which has negatively impacted the material performance. The newly developed HT showed an increase in the number of cycles to failure.

IV. DISCUSSION/CONCLUSIONS

The mechanical testing of traditional, commercially available and newly developed HTs for L-PBF A20X™ were analysed. The comparison test data highlighted the possibility to enhance tensile and fatigue properties of AMed Al alloy through customised heat treatment.

V. FUTURE PLAN/DIRECTION

High-temperature Creep test and HIP HT will be carried out. Furthermore, the correlation between phase evolution and mechanical performance will be assessed.

VI. ACKNOWLEDGEMENT

This work is part of the C-ALM AOHE project funded by the European Union's Horizon 2020 research and innovation programme under grant agreement No 831880.

REFERENCES

[1] P.A. Rometsch, et al., Review of high-strength aluminium alloys for additive manufacturing by laser powder bed fusion, Materials & Design, 219 (2022) 110779.
[2] S.C. Altıparmak, et al., Challenges in additive manufacturing of high-strength aluminium alloys and current developments in hybrid additive manufacturing, Int. j. lightweight mater, 4 (2021) 246-261.
[3] J. Fiocchi, et al., Heat treatment of aluminium alloys produced by laser powder bed fusion: A review, Materials & Design, 204 (2021) 109651.
[4] ECKART. A20XTM - The strongest aluminium alloy. Worldwide! https://eckart.net/de/en/am/a20x

Muhammad Haris
Haris is a Doctoral researcher in Mechanical and Aerospace engineering at Brunel University London, UK. He is based at the National Structural Integrity Research Centre (NSIRC) at TWI, Cambridge, UK. Haris holds an MSc degree and has previously worked on areas related to nanocontainer-based coating in oil and gas industry at the Center of Corrosion Research, Universiti Teknologi PETRONAS, Malaysia. Haris holds a Bachelors degree in Metallurgical Engineering. He is a student member of the Energy Institute, AMPP and IOM3.

Investigating mechanical performance of self piercing rivet (SPR) joint for dissimilar materials joints

Sullivan Smith[1], Lorna Anguilano[2], Ben Robinson[1], Timothy Mitton[2]
[1]TWI Ltd, Granta Park, Great Abington, Cambridge, CB21 6AL, UK
[2]Brunel University London, Brunel University, Kingston Lane, Uxbridge, UB8 3PQ, UK
3rd Year of PhD

Keywords: dissimilar materials, coatings, fasteners, lap-shear test.

I. INTRODUCTION

Self-piercing riveting (SPR) is a mechanical fastening technology used for joining similar and dissimilar materials. In recent years it has been widely employed in automotive and aircraft manufacturing. Consequently, the development of light weight materials has been growing rapidly. These light weight structures are beneficial for both environmental challenges and requires less fuel consumption by reducing the weight of cars, trucks, aircraft, or aerospace vehicles which in turn decreases the fuel consumption of the vehicle resulting in saving money and environment due to less operational costs. The demand of light weight structures is expected to continue as more stringent regulations are expected to reduce the CO2 emission. For example, the UK has set a net-zero target of at least 100% (previously 80%) emission reduction by 2050 [1] which means the progress needs to be accelerated in coming years and lightweight structures will be an integral part for the structural integrity and transportation industry. The use of lightweight materials such as composites and plastics is growing, especially in automotive industry. To be able to join lightweight materials in combination with more traditional materials such as aluminium, steel or alloys etc. current joining techniques must be adapted to be able to join these dissimilar materials. Industries that need to join dissimilar materials are looking for simple and faster techniques of joining them such as self-piercing rivet (SPR) as it offers an ability to join vast similar and dissimilar materials. Furthermore, SPR has the advantages such as no surface preparation or pre-treatment, high joining speed and automation flexibility as compared to other similar joining methods such as resistance welding, friction welding and adhesive joints. Additionally, it can join multiple layers of materials with different thicknesses and can offer better tensile strenght than spot welding due to the formation of interlock between the sheets. In many industrial applications, metal and composites are joined together to achieve desired properties, for example by using fasteners like rivets, adhesives, or bolts. However, it is known that when joining two dissimilar materials it creates a galvanic coupling between two conducting materials in presence of corrosive environment. This occurrence can also be observed when CFRP and other metals or alloys are joined together or simply in contact for a specific time. [2-4].

The research objectives are as follows:

- To experimentally determine mechanical performance of coated rivet joints by using single lap-shear test.

II. DESIGN/METHODOLOGY

A. Joint Preparation:

Dissimilar materials joints were made by joining Aluminium alloy 6061 with Carbon fibre reinforced polymer (CFRP) composites by using Self-Piercing rivet (SPR) joining process. Al alloy sheets were cut using a hydraulic metal shear machine while CFRP sheets were cut by using water jet. A stack thickness of 3.5 mm was achieved by joining two sheets of CFRP and aluminium having thickness of 1.5mm and 2mm respectively. The SPR joint was made by using rivets having shank diameter of 5mm and effective length of 5.5mm. A flat die was used that had a flat bottom surface, a diameter of 10mm, and a cavity depth of 1.2mm. The specimens were prepared using a force-driven electro-hydraulic riveting system. A combination of rivet-die-setting force was used initially and after a series of trials to achieve an optimised joint quality.

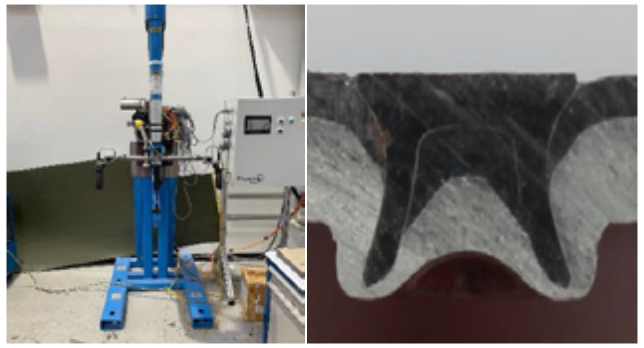

Figure 1. SPR machine (left) Joint made using SPR technique (right).

B. Mechanical test:

The mechanical performance of single-lap joints was evaluated through shear tensile tests both before and after an accelerated corrosion test in the salt spray chamber. A universal testing machine was used to conduct the tests, with a cross-head speed of 3 mm/min.

III. FINDINGS

This study investigated the mechanical performance of SPR joint with coated and uncoated rivet. The test conducted, shows the mechanical performance of SPR joint when coupled with dissimilar materials by using carbon steel rivet. These results will enable us to identify the noble material characteristic in dissimilar materials joints. The obtained trend would identify the effect of coatings on the joint strength in dissimilar material.

IV. CONCLUSIONS

In the current stage, this research is focused in investigating the mechanical strength of SPR-rivet joints when used to join dissimilar materials. It will be interesting to know how rivets coatings behave and can be utilised to understand the degradation of dissimilar material joint.

V. FUTURE PLAN/DIRECTION

The future plan is to study coatings that can be used and protective of rivets while they are used in dissimilar material joints. The joints with different rivets coatings shall be investigated electrochemically and for joint strength.

VI. ACKNOWLEDGEMENTS

This research/publication is made possible by the sponsorship and support of Brunel University London and TWI. This work was enabled through, and undertaken at, the National Structural Integrity Research Centre (NSIRC). This research is funded by TWI's Core Research Programme, a market-driven programme of research and development activities that underpin the creation and optimization of joining, materials, and engineering technologies.

REFERENCES

[1] C. C. Committee. (2021). Progress Report to Parliament. Available: https://www.theccc.org.uk/uk-action-on-climate-change/reaching-net-zero-in-the-uk/.
[2] X. Wu, J. Sun, J. Wang, Y. Jiang, and J. Li, "Investigation on galvanic corrosion behaviours of CFRPs and aluminium alloys systems for automotive applications," Materials and Corrosion, vol. 70, no. 6, pp. 1036-1043, 2019.
[3] M. Shan, K. Guo, G. Gou, Z. Fu, B. Yang, and W. Lu, "Effect of anodizing on galvanic corrosion behaviour of T300 CFRP/5083P-O Al bolted joints," Materials and Corrosion, vol. 71, no. 3, pp. 409-418, 2020.
[4] M. Ostapiuk, M. G. Taryba, L. M. Calado, J. Bieniaś, and M. F. Montemor, "A study on the galvanic corrosion of a sol-gel coated PEO Mg-CFRP couple," Corrosion Science, vol. 186, p. 109470, 2021/07/01/ 2021.

Arunima Bhuvanendran Nair Jayakumari

Arunima joined NSIRC in January 2022 as a PhD student on 'Design of materials and joints for hydrogen service' project at the University of Leicester sponsored by Lloyd's Register Foundation and University of Leicester. The major work on the project is on synthesizing novel alloys for hydrogen service and evaluating its hydrogen diffusivity. Arunima has a background in Chemistry with research experience in synthetic chemistry.

Electrochemical determination of hydrogen diffusion using devanathanstachurski cell

Shiladitya Paul[1],Hong Dong[2]
[1]TWI, [2] University of Leicester
2nd Year of PhD

Keywords: hydrogen embrittlement; hydrogen diffusion; DS-Cell.

I. INTRODUCTION

The ramifications of hydrogen interacting with metals and causing degradation have been a subject of intense research since the late 19th century. Among these topics, Hydrogen Embrittlement (HE) stands out as a widely studied and discussed phenomenon. HE is marked by the deterioration of mechanical properties, specifically the strength and ductility of the material, ultimately culminating in the brittle failure of structural components. In situations where hydrogen is present and can cause damage to materials, it is imperative to devise materials with exceptional mechanical properties that can withstand Hydrogen Embrittlement (HE). A notable contender that has gained significant attention in this regard is high entropy alloys. In general, numerous theories have been put forward by many researchers to explain the mechanism of HE in materials. However, due to the complexity in HE phenomena, the underlying mechanism is still being discussed and extensively reviewed.

To fully understand the mechanism of hydrogen embrittlement, it is required to have a deeper understanding of the ingress of hydrogen into the metals, the transport of hydrogen, the interaction of hydrogen with defects in the crystal lattice and its effect on mechanical properties. With regard to the HE and close connection of it with the fast diffusion of hydrogen, it is crucial in determining the hydrogen diffusivity for developing HE resistant materials. There are various methods for the measurement of hydrogen diffusion in metals and alloys, but an in-situ continuous measurement of hydrogen uptake and diffusion would help in understanding the mechanism and kinetics associated with the process. In the study proposed here would use Devanathan-Stachurski Cell (DS Cell) for hydrogen diffusion measurements of the samples[1].Electrochemical permeation technique using DS Cell have been widely used in various steels, titanium, zirconium and aluminium and nickel alloys and high entropy alloys.

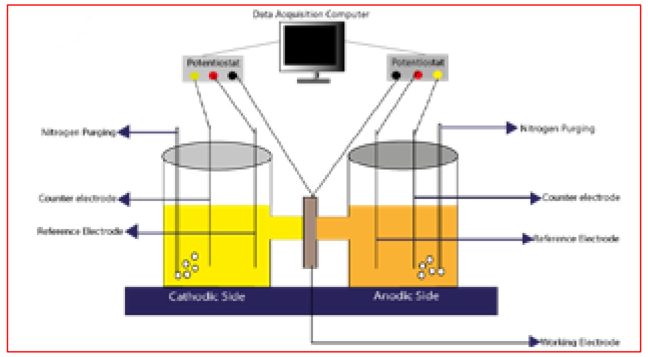

Figure 1. Schematic representation of DS Cell

II. APPROACH

The hydrogen diffusion behaviour of the samples were studied electrochemically using DS-Cell in fig.1. Preliminary hydrogen permeation testing has been conducted according to ASTM G148 on AISI 1010 sheet of thickness 0.30mm as a reference material ground up to SiC 2500 grit. The exposed area of the specimen to the electrolyte on both side of the cell was 3.14 cm^2 .The side of the specimen acted as the cathode was filled with 0.1M NaOH and was galvanostatically polarised at a constant current density of -2 mA/cm^2 using ACM potentiostat. Standard Calomel Electrode [SCE] acted as a reference electrode on both sides and Pt acted as the counter electrode on cathodic as well as anodic side. The anodic side (the hydrogen exit side) was filled with 0.1M NaOH, maintained at a constant potential of +250mV versus (SCE) using ACM potentiostats. Nitrogen was vigorously purged on both the sides throughout the experiments. When the background current was below 0.1$\mu A/cm^2$ in the anodic compartment, electrolyte in the cathodic side was immediately added and the oxidation current was continuously measured in the anodic side and the experiment was repeated twice and diffusion coefficient was calculated. The thermal dependence of the hydrogen diffusion were determined at different temperature [295,310,318K].

III. FINDINGS

The hydrogen permeation curve obtained at 295K for AISI 1010 is given in Figure 2. The methods employed for the diffusion coefficient calculation were time-lag (t_{lag}) method and breakthrough time method(tb), where time-lag point is 63% of the transient and breakthrough time is the time elapsed before the first hydrogen detection on the exit side. The experiment is repeated at different temperatures [295,310,318 K].

Fig:3 shows the influence of temperature on permeation current. In all the three cases the steady state current density increased with increasing temperature and the hydrogen diffusivity increased from 1.39 $\times10^{-12}$ m^2/s at 295 K to 5.57 $\times10^{-12}$ m^2/s. The temperature dependence of diffusivity was fitted using the Arrhenius relationship.

$$D = D_o \exp(-Q/RT)$$

where Do is the temperature independent constant, Q(J/mol) is the activation energy for diffusion which is calculated from the slope of Fig.4 to be 47.064 kJ/mol, where R (J/mol K) is the gas constant and T is temperature in K.

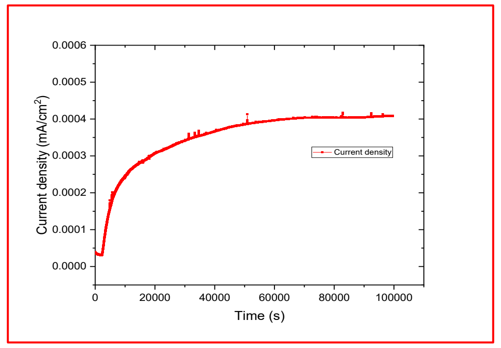

Figure 2. Hydrogen permeation curve of AISI 1010 measured at 295K

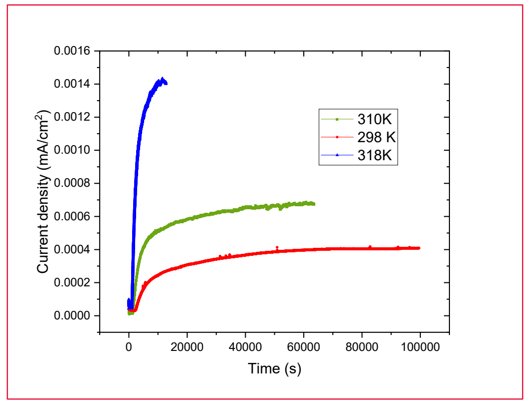

Figure 3. Hydrogen permeation of AISI 1010 measured at 298K, 310K, 318K

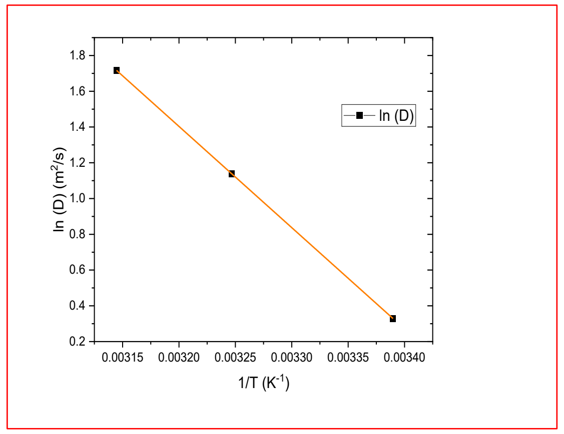

Figure 4. Hydrogen diffusivity evaluated as a function of reciprocal temperature.

IV. CONCLUSIONS

- Hydrogen diffusivity of AISI 1010 mild steel is found to be around 1.56$\times10^{-12}$ m^2/s at 295 K.
- The Arrhenius behaviour of temperature dependence of hydrogen diffusion was verified and the calculated activation energy as 47.064 kJ/mol
- In all the three cases the steady state current density increased with increasing temperature and the hydrogen diffusivity increased from 1.39 $\times10^{-12}$ m^2/s at 295K to 5.57 $\times10^{-12}$ m^2/s at 318K.

V. FUTURE PLAN

The future work consists of synthesising of HEA using arc-melting furnace and its characterization using SEM/XRD and the determination of its hydrogen diffusivity using electrochemical permeation method.

VI. ACKNOWLEDGEMENTS

This publication was made possible by the sponsorship and support of Lloyd's Register Foundation (LRF) and University of Leicester. The work was enabled through, and undertaken at, the National Structural Integrity Research Centre (NSIRC), a postgraduate engineering facility for industry-led research into structural integrity established and managed by TWI through a network of both national and international Universities.

REFERENCES

[1] Devanathan, M. and Z. Stachurski (1964). "The mechanism of hydrogen evolution on iron in acid solutions by determination of permeation rates." Journal of the electrochemical society 111(5): 619.
[2] Cantor, B., et al. (2004). "Microstructural development in equiatomic multicomponent alloys." Materials Science and Engineering: A 375: 213-218.
[3] Yeh, J. W., et al. (2004). "Nanostructured high-entropy alloys with multiple principal elements: novel alloy design concepts and outcomes." Advanced engineering materials 6(5): 299-303.

David Satterlee

David is a second year PhD student at Sheffield Hallam University, having previously completed a bacholars studying Materials Engineering in July 2021. As a PhD student, David is embedded within the team at TWI Sheffield undertaking research using the extreme high-speed laser application process equipment.

The optimisation of Ni superalloy coatings using extreme high-speed laser application (EHLA) technology

Josh Barras[1], Dr Stephen Magowan[2]
[1]TWI Ltd, [2]Sheffield Hallam University
2nd Year of PhD

Keywords: EHLA, LMD, Coatings

I. INTRODUCTION

Improving the corrosion and wear resistance of a component can significantly extend its service life. One solution of improving performance and functionality is through the application of suitable coatings. The requirements of these components (service conditions, regulations, material systems) are continuously evolving. Therefore, the development of new, and optimisation of existing, coating technologies is critical to meet industrial demand for fit-for-purpose coatings, as well as reducing costs (e.g. time, waste) and improving quality/productivity. EHLA is being studied as an alternative to traditional metallic coatings technologies. It has also been specifically developed as a viable alternative to the Hard Chrome Plating (HCP)/Electroplating methods. As a laser deposition technology, there is no exposure to the highly toxic hexavalent chromium produced by the HCP process, a "substance of very high concern" according to the European Chemistry Agency (ECHA) and Registration, Evaluation, Authorisation and Restriction of Chemicals (REACH).

EHLA is an evolution of the laser cladding (LC) process, with a modified powder laser gas jet focus, shown in Figure 1.

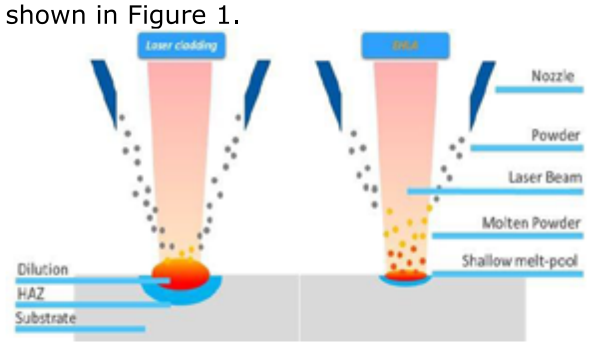

Figure 1: LC and EHLA Comparison [1]

In the EHLA process, powder and a carrier gas are fed into a coaxial nozzle, coincident with a focused laser beam around 1mm above the substrate. This offset allows the powder to melt in-flight, absorbing a significant portion of the laser energy, thus reducing the energy absorbed into the substrate, resulting in reduced dilution and a smaller heat affected zone (HAZ). The pre-melting of the powder removes the dependency of a conventional surface melt pool, required by arc deposition and LC, which allows the process to cover surface at high rates, with deposition speeds up to several hundred metres per minute.

II. DESIGN/METHODOLOGY/APPROACH

In this research, two nickel superalloys have been investigated: Inconel625® (IN625) single-layer coatings; and Inconel718® (IN718) single/multi-layer deposits. The materials have been deposited on austenitic stainless steel (304L) bars and brake discs (shown in Figure 2).

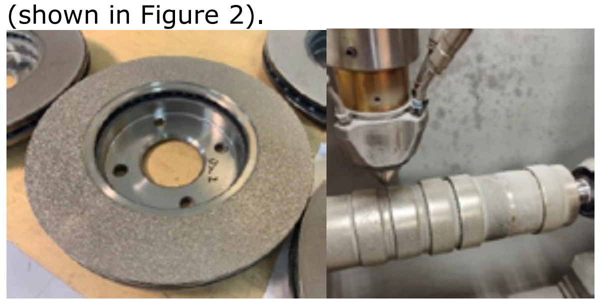

Figure 2: Images of a coated brake disc and bar

The effects of Key Process Variables (KPV), i.e. laser power and powder feed rate, have been evaluated via a series of parametric studies and the Taguchi design of experiments. The deposited coatings were evaluated both microstructurally and mechanically to characterise resultant material properties and derive suitable process windows. Initial characterisation of the deposited samples includes microhardness results, optical microscopy and SEM/EDS analysis.

III. FINDINGS/RESULTS

Through parameter process windows, a region of parameters in which coatings are deposited has been identified via the Taguchi DoE approach (around 50m/min traverse speed, 25g/min powder feed rate, 2kW laser power), see Figure 3. This result has been summarised based on findings of deposits that exhibit low porosity, good interface and surface uniformity, powder efficiency and observed process stability.

Throughout this project, single-layer IN625 coatings have typically been measured between 50 and 500µm. For the IN718, where multi-layer approaches have been used, samples could be produced without any major issues at 10-20 times this thickness, depending on the number of layers deposited.

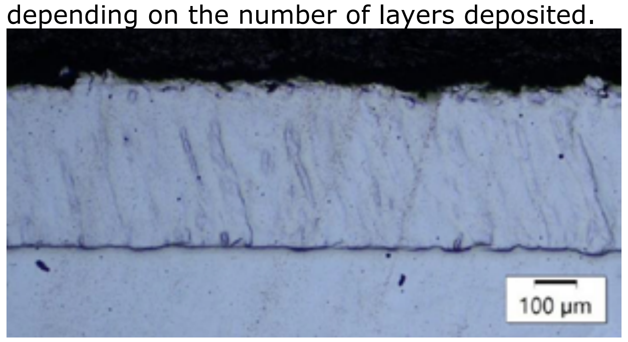

Figure 3: Image of a good quality 400µm IN625 EHLA coating (2.25kW, 65m/min, 25g/min)

Early assessment of the developed coatings, in terms of coating thicknesses and visual integrity, indicate that with further testing EHLA could be validated as a sensible alternative to HCP. Figure 4 shows typical thicknesses and heat input of metallic coating technologies. EHLA is not included in the diagram, however the low temperature and coatings of over 50µm dictate a similar area to Electroplating.

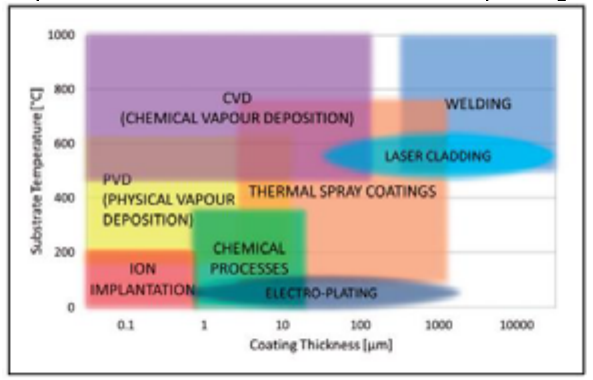

Figure 4: Comparison of coating technologies with regards to temperature imparted upon the substrate and resultant coating thickness [2]

IV. DISCUSSION/CONCLUSIONS

The project work so far upon EHLA has demonstrated:

- The process produces low dilution; however, we have been unable to quantify this yet.
- Above 2.5kW, coatings exhibited low porosity but the process risks instability and clogging of the nozzle, more work needs to be conducted in future to resolve this, nozzle positioning and powder jet stream to beam diameter optimisation may enable higher powers.
- The nozzle's stand-off distance is important, targeted 10mm above the substrate (1mm above the powder jet stream focus).
- For multi-layer depositions solid bars are the preferred substrate option to ensure minimal distortion, dwell times have also been introduced to reduce the effect of heat applied.
- Porosity, though not quantified, has been viewed as minimal throughout, however lack of fusion is common in the multi-layer builds.

Through these parametric studies, the EHLA process has been shown to deposit single-layer coatings to near target thicknesses, with optimisation required for repeatability. Multi-layer coatings require further optimisation and understanding on deposition behaviour and mechanical properties, providing a baseline to assess suitability for conventional Additive Manufacture (AM) and repair applications.

V. FUTURE PLAN/DIRECTION

The main focus for the future is the ongoing development of methods of best practice for the EHLA process, from deposition to analysis, an aspect requested by industry but has minimal published evidence for as a new technology. Another goal for future work is the assessment of the repeatability of the process using the same parameters, establishing reliability at producing similar coatings each time (i.e., thicknesses, porosity, microstructure, dilution). The future testing/evaluating for both powders will include surface roughness measurements, as well as interface assessments and bond strength tests. Beyond that, to better understand the performance of the EHLA-deposited single-layer IN625, a series of corrosion resistance tests will be undertaken to provide evidence of suitability for industrial use. The single-layer IN625 coating will be benchmarked against existing industrial coating technologies, e.g., High-Velocity Oxy-Fuel thermal spray (HVOF). For IN718 multi-layer studies, the next step will be industry-used AM quality methods, i.e., tensile tests.

VI. REFERENCES AND ACKNOWLEDGEMENTS

[1] TWI Ltd. (n.d.). What is Extreme High Speed Laser Application (EHLA)? Retrieved from TWI Global: https://www.twi-global.com/technical-knowledge/faqs/what-is-ehla.

[2] Christoforou, P., Dowding, R., Pinna, C., & Lewis, R. (2021). Two-layer laser clad coating as a replacement for chrome electroplating on forged steel. In I. o. Engineering, Journal of Mechanical Engineering Science, Volume 235, Issue 23 (pp. 7120-7138). Institute of Mechanical Engineering.

This publication was made possible by the sponsorship and support of CRP. The work was enabled through, and undertaken at, the National Structural Integrity Research Centre (NSIRC), a postgraduate engineering facility for industry-led research into structural integrity established and managed by TWI through a network of both national and international Universities.

Magali Rego

Magali is a 3rd year PhD Candidate at The Open University in Milton Keynes and TWI in Cambridge, with funding from Lloyd's Register Foundation. Before moving to the UK, Magali studied Biochemistry (BSc) and Chemical Analysis and Characterization Techniques (MSc) in Braga (Portugal) at the University of Minho. Magali has previous experience working in industrial research projects at Continental ITA and INL developing environmentally friendly and nanoparticle based coating solutions for textile and wood innovative applications. Her PhD project focuses on developing a chemical design approach to allow the regeneration of the precursor materials of epoxy thermoset into a closed-loop recycling cycle.

Introduction of solvent de-curing trigger to enable dissolution of epoxy thermoset

James Bruce[1], Peter Taylor[1], Alan Taylor[2]
[1]School of Life, Health and Chemical Sciences, The Open University, [2]TWI
3rd Year of PhD

Keywords: epoxy thermoset, recycling, silica, composites, de-curing trigger

I. INTRODUCTION

Current methods to recycle epoxy thermoset resin (widely used in high performance composites in the aerospace, automobile and renewable energy industries) are immature and have room for improvement. Epoxy thermoset resins, regarded as unrecyclable plastics [1], have a highly crosslinked three-dimensional network and cannot be remolded like thermoplastics, which makes it quite a challenge to enable monomer recovery. Current mechanical and chemical recycling methods cause a downward cycle for products reuse, leading to a decrease of the quality and value of recovered products such as glass and carbon fibres. If not meeting the required quality and mechanical requirements of the reused product, these recovered materials are typically disposed of via pyrolysis or in landfill sites. Whilst chemical recycling is considered promising because it can produce useful chemicals and potentially achieve upcycling, some approaches use toxic solvents at dangerously high temperatures, such that the process is difficult to scale up, with waste and by-products disposal that are harmful for the environment. [1]

Aligning with The European Union initiatives for more plastics to be included in a circular economy strategy, the idea of achieving an epoxy thermoset closed-loop recycling using silica as a recoverable monomer is one possible solution to the main limitations faced so far. To achieve this, a reversible linking structure must be planned and functionalised onto the surface of the silica, so it is compatible with the thermoset resin, and it is sensitive to a specific chemical stimulus to incite de-curing.

II. METHODOLOGY

The methodology was established by following a structured chemical design plan, entailing the following steps: (1) Introduction of labile chemical groups onto silica, (2) Compatibilisation of surface chemical groups with epoxy system, and (3) Functionalised silica incorporation into an epoxy resin system.

The surface of the selected silica is modified with a reactive group for step (1), this group is further reacted in step (2) with a thiol-amine molecule. For step (3), the amino functionalised silicas are washed and dried to a fine powder and directly dispersed into an epoxy resin with help of a Speed mixer. They were tested for dispersion and gelation at room temperature before heat curing with commercial epoxy DER332.

For step (1) and (2), Drop Shape analysis (DSA) was used as an unconventional technique to assess chemical surface modification. For step (3), Differential Scanning Calorimetry (DSC) was the chosen method to study reactivity and determine heat cure temperatures.

III. RESULTS

The novel powders with built-in de-curing trigger produced from step (2) were further analysed with DSA to determine changes in surface wetting caused by the chemical functionalisation protocols. Pyrogenic silica has an hydrophilic surface behaviour when tested as a packed powder. When this pyrogenic silica is functionalised in step (1) the surface chemistry is modified to exhibit lyophobic behaviour when exposed to solvents with different surface tensions (Figure 1), mainly due to the presence of methyl ($-CH_3$) groups on the surface.

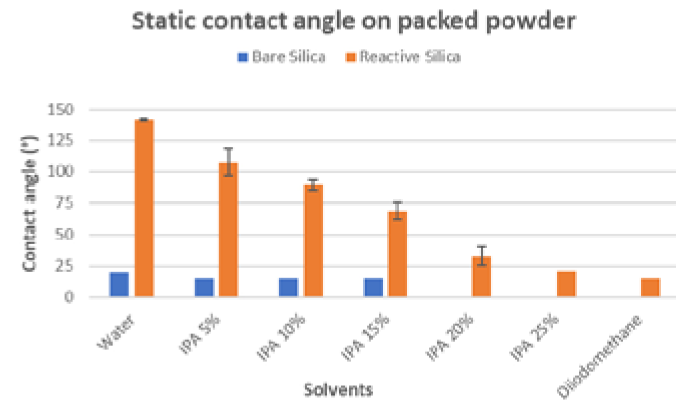

Figure 1 Static contact angle measurements on packed powder over 5 minutes of continuous exposure to 10μl drops of different solvents

In step (3), the reactive silica is functionalised with thiol-amine groups to an amino functionalised surface and changes back to being hydrophilic, mainly due to the presence of amine groups on the surface. Recorded videos of wetting behaviour prove these phenomena.

For step (3), amino functionalised silica powders were loaded into epoxy DER332 to obtain visual proof of gelation occurring over a 2-week period. In Figure 2, gelation can be seen on the right side where 5% amino functionalised silica was mixed with epoxy DER332, indication that reaction between amine and epoxy groups has occurred at room temperature.

Figure 2 Visualization of epoxy gelation in transparent vials. On the left epoxy DER332 was mixed with reactive silica (non-reactive with epoxy) and on the right with amino functionalised silica (reactive with epoxy)

To determine the optimum temperature for the epoxy/amino functionalised silica mixtures to cure, the reactivity between the amino functionalised silica powder and epoxy DER332 were assessed using DSC analysis. DSC curves in Figure 3 shows the exothermic peaks appearing at different temperatures (125 ºC and 200 ºC), indicating that overtime, the amine groups on the silica powder reacted with the epoxide groups from the resin, although this needs to be studied further.

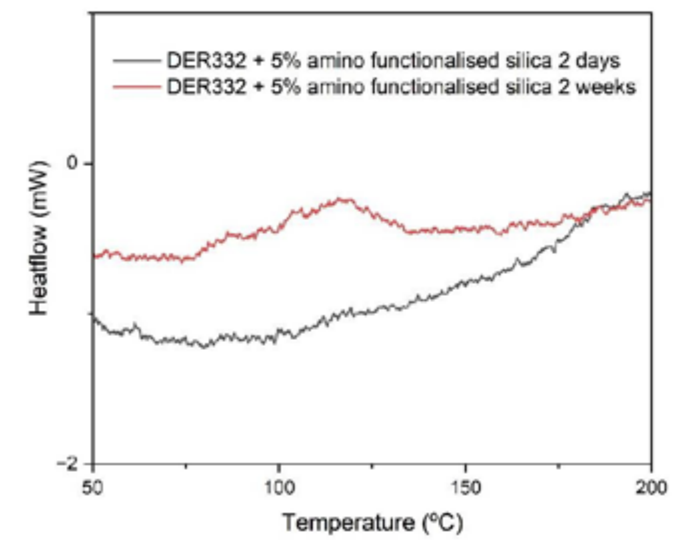

Figure 3 Non-isothermal DSC curves of epoxy resin DER332 loaded with 5%(w/w) of amino functionalised silica, after being mixed and let to react for 2 days and 2 weeks

IV. CONCLUSIONS

The new amino functionalised silica powders proved to be interacting with the epoxy resin. Reproducible functionalisation of amino functionalised silica is possible with a simple and scalable process from 100 milligrams to 100 grams. This achievement of controlled functionalisation of the silica additives and fine tuning the resultant surface properties leads to a versatile recoverable monomer, which whilst being a complex task has great value and potential.

V. FUTURE PLAN

Further ahead in the project, these novel materials will need to be heat cured in a proper silicone mould and validated against the current state-of-the-art. The next challenge will be to decure them and prove that the silica and epoxy monomers can be recovered, closing the gap that separates these unrecyclable plastics from their full use in a closed life material cycle.

VI. ACKNOWLEDGEMENTS

This publication was made possible by the sponsorship and support of Lloyd's Register Foundation. The work was enabled through, and undertaken at, the National Structural Integrity Research Centre (NSIRC), a postgraduate engineering facility for industry-led research into structural integrity established and managed by TWI through a network of both national and international Universities.

REFERENCES

[1] X. Zhao, X. Liu, K. Feng, W.-L. An, F. Tian, R. Du, S. Xu, L. Chen, G. Wu, Y.-Z. Wang, "Multicycling of Epoxy Thermoset Through a Two-Step Strategy of Alcoholysis and Hydrolysis using a Self-Separating Catalysis System", ChemSusChem 2022, 15, e202101607, doi: 10.1002/cssc.202101607.

Adriana Castro-Vargas

Adriana joined NSIRC in January 2021 as a PhD scholar on the ProCoat project at the University of Leicester sponsored by Lloyd's Register Foundation. Adriana has a background in Metallurgy and Materials Science. She has carried out research and teaching in Materials Engineering. Her research is focused on determining the damage tolerance of sacrificial coatings used in the offshore wind turbines.

Real-time optical and electrochemical monitoring of extreme damage tolerant sacrificial coatings

Shiladitya Paul[1], Simon Gill[2]
[1]TWI, [2]University of Leicester
3rd Year of PhD

Keywords: Damage Tolerance, Real-time Optical Inspection, Thermal spray aluminium

I. INTRODUCTION

Thermally sprayed aluminium (TSA) is widely used as a sacrificial coating in marine environments. It can provide cathodic protection to steel even if damage occurs during installation because TSA is more galvanically active than steel. Most studies have focused on evaluating minor defects (1-5% of exposed steel). However, the level of damage that TSA can tolerate remains scarce in the literature. A few studies have reported the ability of TSA to protect steel when the area of exposed steel is greater (up to 18% and 90%) [1,2]. This work seeks insight into the protection mechanism provided by TSA in the presence of extreme damage by using an innovative methodology consisting of a real-time inspection of the surface activity and a simultaneous record of the evolution of the open circuit potential (OCP).

II. DESIGN/METHODOLOGY/APPROACH

BS EN S355J2 C-Mn steel coupon of dimensions 75 mm x 75 mm x 6 mm was cut, and the surface was prepared by grit blasting to the standard cleanliness of Sa 3. The coating was obtained by twin-wire arc spray process (300 µm thick, 1050 aluminium alloy). First, an intentional defect (blind hole) 0.8 mm deep and 25.2 mm diameter was machined with a flat slot drill in the centre of the coupon, followed by inserting a threaded rod into the top of the coupon to make the electrical connection. Real-time inspection of damaged TSA in synthetic seawater was conducted using an optical-electrochemical cell (Correlimage® and image recognition software). The incorporated camera in the cell allowed to capture the surface activity in the coated region and on the exposed steel (sequential images every 2 h) from the start of the immersion until 30 d of exposure. Simultaneously, the evolution of the open circuit potential (OCP) against Ag/AgCl (Sat. KCl) reference electrode at room temperature (18±2°C) and stagnant conditions was performed using a VSP 300 Biologic potentiostat. The exposed surface area to synthetic seawater is only 10 cm^2; therefore, the defect dimension (exposed steel) represents 50% of the total surface under study. Figure 1 illustrates the experimental setup. After the test, the characterisation of the samples was performed by visual inspection, Scanning Electron Microscopy (SEM) and Energy Dispersive X-ray spectroscopy (EDX).

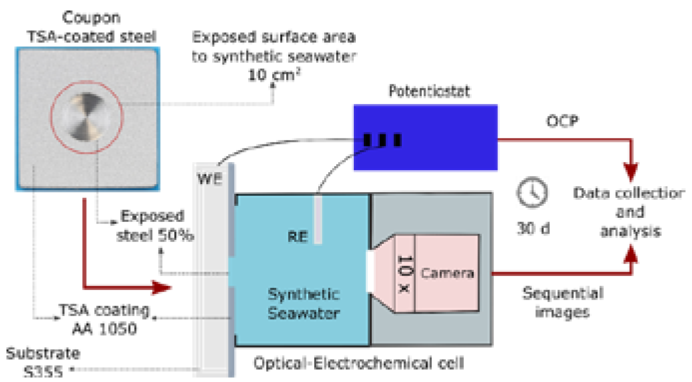

Figure 1. Schematic representation of in situ optical and electrochemical monitoring of TSA with 50% damage.

III. FINDINGS/RESULTS

The optical-electrochemical monitoring of TSA with 50% of exposed steel is shown in Figure 2. The most representative images were included and correlated with OCP changes (original image on the left and processed image on the right). The scale from royal blue to red colour denotes the surface activity.

At the beginning of the immersion, the potential was -0.71 V and decreased rapidly in the next few hours. Slight signs of rust were observed in the exposed steel because the system reached the recommended protective potential for steel (-0.743 V according to DNV-RP-B401) only after 3 h. The potential was -0.87 V after 1 day of the test, and the aluminium surface became progressively activated due to the degradation of the air-formed oxide layer. Furthermore, the roughness and porosity of the coating lead to non-uniform wettability. Bubbling was observed in the exposed steel and coating after 2 d of immersion (-0.98 V). This can be attributed to hydrogen generation in the water reduction reaction and aluminium dissolution typical in these systems [1]. The evolution towards more positive potentials after 4 d of immersion (-0.96 V) is directly associated with forming a layer of calcareous deposits (optically recognisable) on the exposed steel. The potential reached a stable value, around -0.95 V. The surface activity remained very low, as observed in the processed images from day 23 to day 30. It can be seen in the image after 30 days of exposure that the calcareous deposits are located preferentially in the lower area of the defect; they also dislodged and accumulated at the bottom of the tank. No corrosion was seen in the defect area after the test.

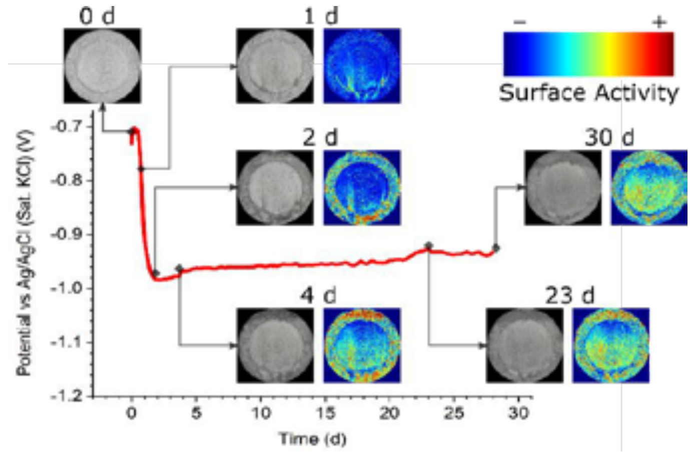

Figure 2. OCP evolution of TSA with 50% damage and its correlation with surface activity.

Figure 3 shows the SEM images from the top view of the defect. Two structures represented by letters A and B can be clearly observed. EDX analysis found that zone A contains Mg-rich compounds and zone B contains Ca-rich compounds. Magnesium hydroxide crystallizes in one form, brucite, which corresponds to zone A. Figure 3b shows the typical cauliflower or needle morphology (zone B) of the allotropic form of calcium carbonate, known as aragonite [3].

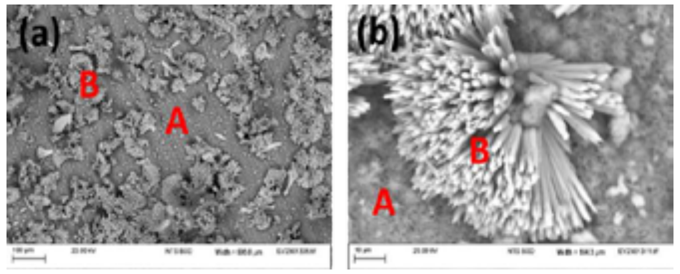

Figure 3. SEM images of the exposed steel. Mg-rich compounds in zone A. Ca-rich compounds in zone B. (a) 400 x. (b) 1000 x.

IV. DISCUSSION/CONCLUSIONS

- The aluminium surface gradually activated until the air-formed layer degraded. This activation occurs during the first few hours of the immersion and is related to the potential drop.
- The evolution of the potentials towards less negative values after 2 d of exposure is directly associated with the precipitation of a layer of calcareous deposits on the exposed steel.
- The stabilisation of the potential and low surface activity recorded by the image recognition software corroborates the barrier properties of calcareous deposits, adding protection to the exposed steel.
- No corrosion or rust was visible to the naked eye in the defect area after exposure, providing evidence of the excellent damage tolerance of TSA, even in the presence of extreme damage.

V. FUTURE PLAN/DIRECTION

The effect of seawater flow on the performance of damaged TSA coating will be addressed in the next stage of this investigation.

VI. ACKNOWLEDGEMENTS

This publication was made possible by the sponsorship and support of Lloyd's Register Foundation (LRF) and University of Leicester. The work was enabled through, and undertaken at, the National Structural Integrity Research Centre (NSIRC), a postgraduate engineering facility for industry-led research into structural integrity established and managed by TWI through a network of both national and international Universities.

REFERENCES

[1] S. Paul, "Cathodic Protection of Offshore Structures by Extreme Damage Tolerant Sacrificial Coatings," NACE International Corrosion Conference & Expo, paper no. 10949 (2018), p. 1-12.
[2] Paul, Shiladitya. "Effect of Damage on the Corrosion Performance of Thermal Spray Aluminium (TSA) Coating in Synthetic Seawater." Applied Sciences 13.2 (2023): 1109.
[3] Carré, Charlotte, et al. "Electrochemical calcareous deposition in seawater. A review." Environmental Chemistry Letters 18 (2020): 1193-1208.

nsirc

ENQUIRIES@NSIRC.CO.UK
+44 (0) 1223 899 000
WWW.NSIRC.CO.UK/CONFERENCE2023

Students Soumyadeep Datta (left) and Ana Araujo-Lascano working in the Brunel Innovation Centre laboratory at TWI in Cambridge, UK.
Photo: Lloyd's Register Foundation / Sam Baker Photography